primarily composed of two modules corresponding to the intestinal lumen and body. Between these modules, it is enough to pass only the value of an intestinal drug absorption rate. To ensure maintainability and scalability of the model, these modules were capsuled to hide unnecessary values, and opened with only a port to pass the absorption rate value. By connecting the ports with an edge, these capsule modules can communicate with each other. Each module was further modeled in a hierarchical manner. Using a template/instance framework of PHML, the absorption rate was calculated in the intestinal lumen module by summing up the values from each of the instances corresponding to multiple doses. The body module includes the functional modules for the liver and blood, in addition to a module for common static variables. Differential equations and variables were implemented in the liver and blood modules. Upon developing PBPK models for an inducer and a CYP3A4 substrate drug, the models were bridged with a capsuled functional module for induction of CYP3A4 (Fig. 1B). The CYP3A4 induction module receives the unbound concentration of the inducer in the liver from the inducer PBPK model and provides the *IR* value for the substrate PBPK model. However, the module was simply a frame, and its object was implemented in a SBML format. Fig. 1C represents a SBML model for induction of CYP3A4 developed using CellDesigner.

Results

Modeling of CYP induction dynamics

The pooled data set obtained from 24 different sources comprised 43 and 40 data points for CYP3A4 enzyme activity and mRNA expression levels, respectively. Considering the effect of inter-donor variability on the baseline level of CYP3A4 activity, an extended least square analysis was performed based on Eqs. 6–8 (see Methods). The parameters EC_{50}, k_{inact}, $k_{rna,deg}$, $k_{cyp,deg}$, p and q were estimated to be 1.18 μM, 0.0530 h^{-1}, 0.0282 h^{-1}, 0.313, and 4.34, respectively, in addition to the inter-donor variability of CYP_0 (ω^2) of 0.318. Interestingly, the $k_{cyp,deg}$ estimated was comparable to the one that was previously optimized for better *in vitro/in vivo* extrapolation (0.03 h^{-1}) [51,52]. Fig. 2 represents simulated surface plots for mean CYP3A4 activity and mRNA expression as a function of concentration and time. Expression of mRNA reached a maximum level at ~40 h following the onset of incubation with rifampicin, whereas the peak of CYP3A4 activity induction was delayed in comparison.

The data set for induction of CYP3A4 activity was also analyzed based on a conventionally used indirect effect model. However, simultaneous estimation of all parameters by curve fitting failed, probably because estimation of k_{deg} requires a clear observation of the maximally induced state in the profile. Alternatively, using the k_{deg} value from the literature [51,52], the EC_{50} and E_{max} values were estimated by curve-fitting. When the k_{deg} value was a default value of the Symcyp simulator (0.0072 h^{-1}), the EC_{50} and E_{max} values were estimated to be 0.283 μM and 37.1, respectively, in addition to a ω_{Emax}^2 of 0.726. When the k_{deg} corrected for more accurate *in vitro-in vivo* extrapolation (0.03 h^{-1}) [51,52] was used, the EC_{50} and E_{max} values were estimated to be 0.269 μM and 16.7, respectively, in addition to a ω_{Emax}^2 of 0.702.

When the analysis based on a simple static model was performed using only 72-h data, the EC_{50} and E_{max} values were estimated to be 0.281 μM and 14.8, respectively. The ω_{Emax}^2 value was 0.874.

Modeling of the clinical pharmacokinetics of rifampicin

Blood concentration-time profiles following repeated oral administration of rifampicin were simultaneously analyzed to estimate its pharmacokinetic parameters based on a simplified PBPK model. The estimated k_a, V_1, K_m, $K_{p,h}$, k_{in}, k_{out}, and F values were 0.963 h^{-1}, 17.2 L, 0.370 mg/L, 10.6, 0.0193 mg/h, 5.75×10^{-4} h^{-1}, and 8.64 L/mg, respectively. Fig. 3 represents simulation curves for the blood concentration of rifampicin when using different oral doses, together with experimentally obtained values. To confirm the nonlinearity of rifampicin pharmacokinetics, AUC_{0-12h} for 300 mg b.i.d. (twice a day) and 600 mg q.d. (once a day) were calculated (Fig. 4). Even though the total daily dose is the same, the AUC_{0-12h} for 300 mg b.i.d. rifampicin was much smaller than that for 600 mg q.d. This result could be successfully explained by considering it to be a saturable elimination process. Auto-inducible elimination of rifampicin was described by a concentration-dependent increase in V_{max}.

In vitro-in vivo extrapolation

Using Eqs. 15–17, the concentration of unbound rifampicin in the liver was computed. The profile was convoluted into Eq. 6 to estimate CYP3A4 induction under clinical conditions, assuming that the mechanism of CYP3A4 induction is equivalent between *in vitro* and *in vivo* states. Fig. 5 shows a simulation of CYP3A4 induction following repeated oral dosing of rifampicin. The level of CYP3A4 activity was transiently increased, peaking on day 4, and then stabilizing on day 6 or later. Fluctuation of CYP3A4 activity arising from repeated dosing of rifampicin was minimal, unlike that of the blood concentration of the drug. Therefore, a static model for enzyme induction would be sufficient to describe the DDI occurring after rifampicin has been repeatedly administered for more than 5 days.

Table 1 summarizes clinical DDI results between rifampicin and drugs known to be metabolized by CYP3A4. The *IR* values were estimated as an average of CYP3A4 activity induction for the day studied, according to the dose, dosing interval, and number of days treated with rifampicin. Using *IR* and fm_{CYP3A4} for each drug, reduction of *AUC* because of co-administration of rifampicin was calculated and compared with clinical data (Fig. 6). The predictive correlation coefficient (Q^2) and standard deviation of prediction errors (*SDEP*) were 0.684 and 0.0630, respectively. Thus, the reduction of *AUC* for various drugs was predicted with fairly good accuracy when using *in vitro* parameters for CYP3A4 induction.

For comparison, prediction using an indirect effect model was conducted. When the default k_{deg} value of the Simcyp simulator (0.0072 h^{-1}) and its corrected value for an *in vitro-in vivo* correlation (0.03 h^{-1}) were used [51,52], the Q^2 values were 0.499 and 0.570, respectively. In addition, the Q^2 values were estimated to be 0.604 when the prediction was made by a simple static model, where the average concentration of rifampicin in blood was calculated by dividing its *AUC* by the dosing interval (i.e., 24 h). The predictions provided by both cases were not as accurate as the presently proposed model.

Simulation of non-steady state DDI using the PHML model

Taking alprazolam as an example, of which the DDI was investigated under short-term treatment with rifampicin, the early phase of DDI was simulated. PBPK parameters for alprazolam (see Table S2) were obtained by curve-fitting to its blood concentration profile as has been reported previously [7], and PBPK models for alprazolam and rifampicin were implemented in PHML using PhysioDesigner. Fig. 7A shows simulations of the blood concentration of alprazolam in the presence and absence of co-administration of rifampicin. Both drugs were assumed to be

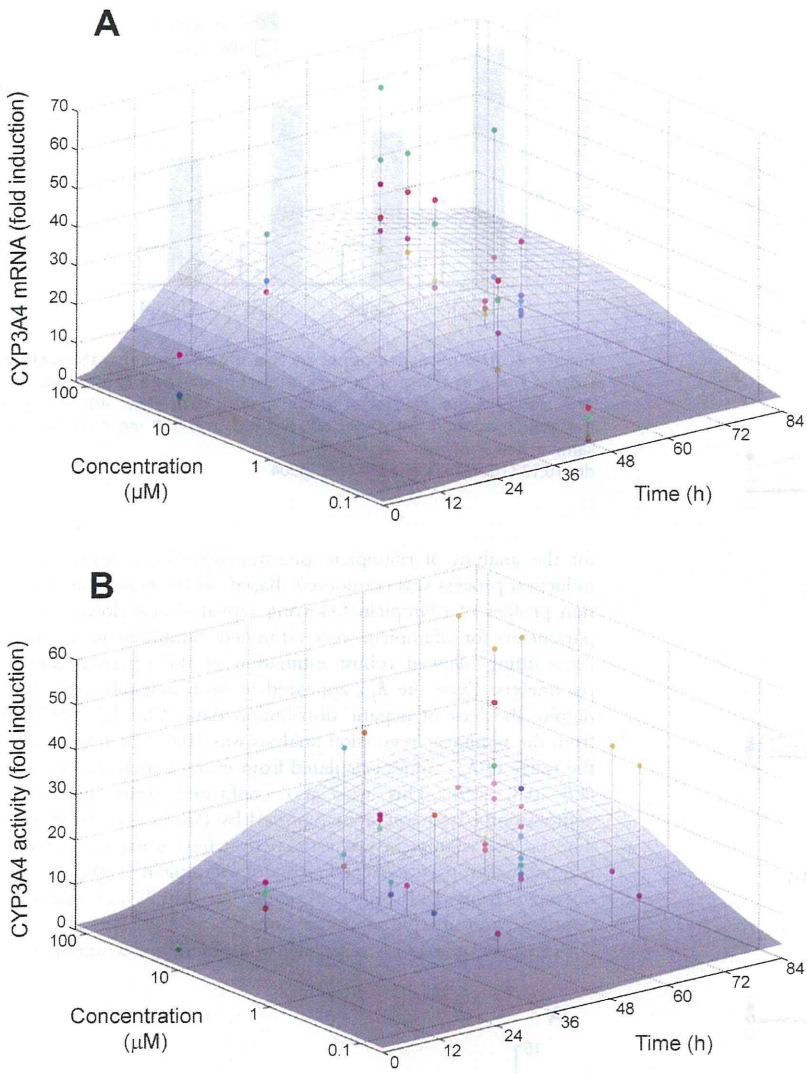

Figure 2. Curve-fitting to experimental data of the induction of CYP3A4 by rifampicin in human hepatocytes. Fig. 2A represents the relative fold induction of CYP3A4 mRNA, while Fig. 2B represents that of the protein level determined by enzyme activity measurements. The data for each donor is presented in a different color. The baseline-normalized data and corresponding equations, i.e., Equations 6–8, were used for this analysis, assuming that inter-individual variability for induction is because of differences in baseline CYP3A4 activity. The surface curves represent the averages.
doi:10.1371/journal.pone.0070330.g002

administered orally every 24 h. In the absence of rifampicin, the blood concentration of alprazolam was increased stepwise following repeated oral doses and eventually reached a steady state. In contrast, in the presence of rifampicin the blood concentration of alprazolam decreased in a time-dependent manner and then reached a steady state at the lower level. Fig. 7B represents comparison between simulation results and measured clinical data [35]. The concentration profile of alprazolam with rifampicin treatment was predicted well (*SDEP*: 0.760), using pharmacokinetic parameters of both drugs and induction dynamics parameters for rifampicin. Pharmacokinetics of other drugs with relatively shorter-term rifampicin treatment were also simulated (see Figure S1), if the time-course data were available.

Discussion

Rifampicin is a strong inducer of drug metabolizing enzymes such as CYP3A4. Rifampicin binds to the nuclear receptor pregnane X receptor (PXR). Once activated, PXR forms a heterodimer with the retinoic receptor (RXR), translocates into the nucleus, and acts as a transcriptional factor. Transactivation of PXR by rifampicin is regulated in a complex manner. Rifampicin-activated PXR is negatively regulated by the small heterodimer partner (SHP), which can be induced by farnesoid X receptor (FXR) ligands [53]. SHP was shown to prevent the PXR/RXR heterodimer from binding to DNA in a pull-down assay, while over-expression of SHP inhibited transactivation of PXR by rifampicin [53]. However, rifampicin-activated PXR is known to suppress expression of the SHP gene, while simultaneously

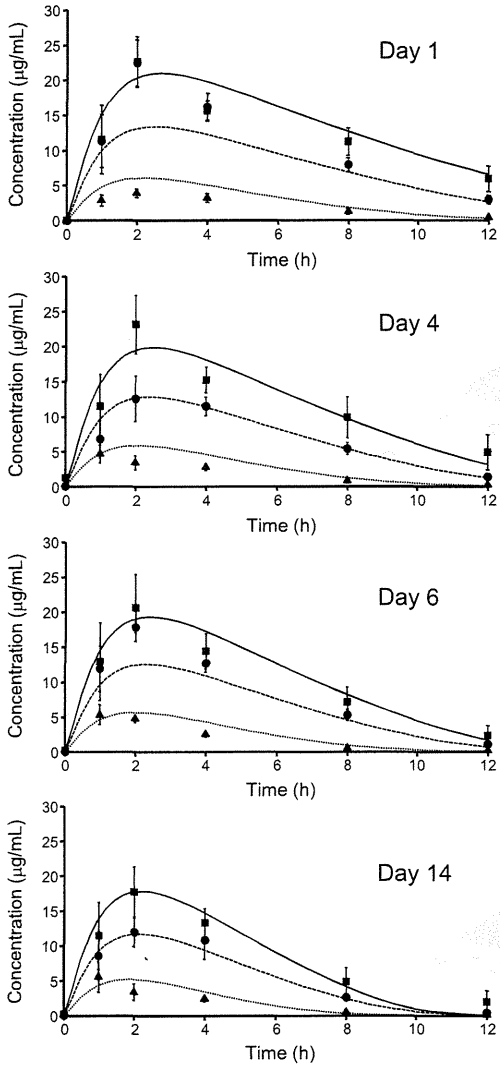

Figure 3. Nonlinear curve-fitting to the blood concentration of rifampicin with repeated oral administration. Clinical data measured on day 1, 4, 6, and 14 (Ref. 40) were simultaneously analyzed based on a PBPK model considering an auto-inducible metabolic process (Eqs. 15–17). Theoretical curves are represented for each data set. Keys: 300 mg, b.i.d. (▲, dotted line); 600 mg, q.d. (●, broken line); 900 mg q.d. (■, solid line).
doi:10.1371/journal.pone.0070330.g003

interacting with HNF4α, SRC-1 and PGC-1α to initiate transcription of the CYP3A4 gene [54]. As shown in Fig. 2, the levels of CYP3A4 mRNA post administration of rifampicin (using data compiled from the literature), appear to be highest at around 48 h. In the present analysis, these observations were regarded as a consequence of gene expression regulatory networks and were described using a simplified negative feedback model.

It has been observed that upon repeated oral administration, the clearance of rifampicin increases because of self-induced metabolism [41,47]. Since the enzyme responsible for the metabolism of rifampicin has recently been identified [55], it is still unclear whether its expression can be induced by a PXR-mediated mechanism, similar to CYP3A4 and other drug metabolizing enzymes [56–58]. Therefore, in order to construct a PBPK model

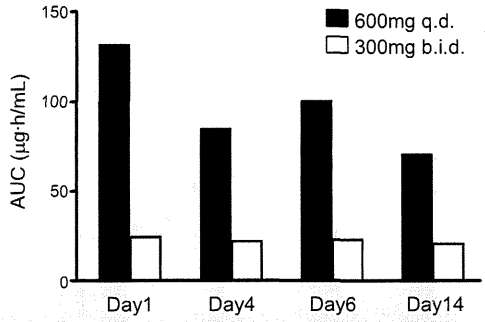

Figure 4. *AUC* measurements of the blood concentration-time profile for oral rifampicin with different dosage regimens. The *AUC* values were calculated from clinical data (Ref. 40) using a trapezoidal method. Note that 600 mg q.d. and 300 mg b.i.d. are the same in terms of total daily dose.
doi:10.1371/journal.pone.0070330.g004

for the analysis of rifampicin pharmacokinetics, a simple auto-induction process was considered. Based on the blood concentration profiles of rifampicin following repeated oral dosing, seven parameters for rifampicin were estimated. Simultaneous multiple curve-fitting allowed robust estimation of the pharmacokinetic parameters. Even the $K_{p,h}$ appeared to be reasonably estimated, despite the lack of hepatic distribution data. The $K_{p,h}$ obtained from the nonlinear regression analysis was 10.6, which fell within the range of $K_{p,h}$ values calculated from *in vivo* human biopsy data (4.8–30.3) [59]. This was also confirmed using the tissue composition-based equations reported by Poulin and Theil [60]. The $K_{p,h}$ for rifampicin was estimated at 6.01 using a computed octanol/water partition coefficient for rifampicin ($\log K_{ow}$: 4.24, obtained from EPI Suite, available at http://www.epa.gov/opptintr/exposure/pubs/episuite.htm).

In vitro parameters for rifampicin were estimated assuming that

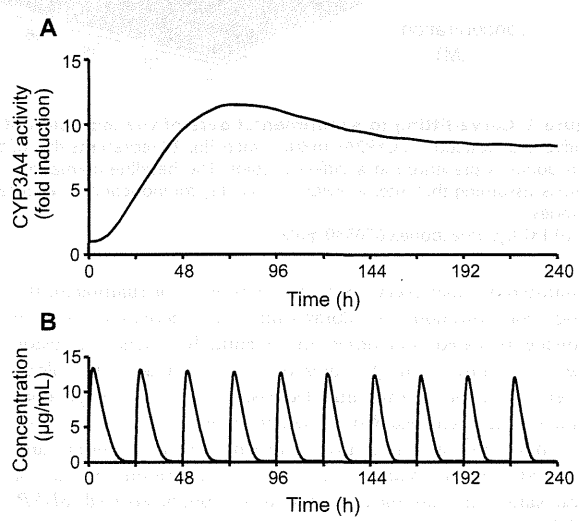

Figure 5. Simulation of the induction of CYP3A4 following repeated oral dosing of rifampicin. Fig. 5A represents the relative fold induction of CYP3A4 enzyme activity, while Fig. 5B represents the blood concentration of rifampicin following oral dosing of 600 mg q.d.. Equations 6–8 and 15–17 were used for this simulation.
doi:10.1371/journal.pone.0070330.g005

Table 1. Prediction of DDIs for various CYP3A4 substrate drugs with concomitantly administered rifampicin.

Substrate		clinical DDI[b]				predicted DDI[c]	
name	fm_{CYP3A4}[a]	daily dose of rifampicin (mg)	days	AUC ratio	Ref. ID	induction ratio (IR) of CYP3A4 activity	AUC ratio
alprazolam	0.75	450	4	0.12	35	9.25 (6.51–19.0)	0.14
atorvastatin	0.68	600	5	0.20	25	9.64 (6.81–19.7)	0.15
buspirone	0.99	600	5	0.088	28	9.64 (6.81–19.7)	0.10
cyclosporine	0.80	600	11	0.27	36	8.16 (5.81–16.5)	0.15
gefitinib	0.39	600	16	0.17	31	7.68 (5.48–15.5)	0.28
imatinib	0.28	600	11	0.26	26	8.16 (5.81–16.5)	0.33
mefloquine	0.44	600	7	0.32	38	8.63 (6.14–17.5)	0.23
midazolam	0.92	600	5	0.041	40	9.64 (6.81–19.7)	0.11
midazolam	0.92	600	9	0.12	27	8.36 (5.94–16.9)	0.13
nifedipine	0.78	600	7	0.082	37	8.63 (6.14–17.5)	0.14
prednisolone	0.18	480	30	0.49	30	6.55 (4.71–13.1)	0.50
simvastatin	1.00	600	9	0.090	27	8.36 (5.94–16.9)	0.12
simvastatin	1.00	600	5	0.14	29	9.64 (6.81–19.7)	0.10
telithromycin	0.49	600	7	0.14	39	8.63 (6.14–17.5)	0.21
triazolam	0.93	600	5	0.051	34	9.64 (6.81–19.7)	0.11
zolpidem	0.40	600	5	0.28	33	9.64 (6.81–19.7)	0.22
zopiclone	0.44	600	5	0.18	32	9.64 (6.81–19.7)	0.21

a) Fraction of the drug metabolized by CYP3A4 (fmCYP3A4) and clinical DDI data were taken from the article of Ohno et al. [24].
b) Clinical data were obtained from the articles shown with the reference ID (Ref. ID).
c) Induction ratio (IR) of CYP3A4 activity was calculated from daily dose and days of administration of rifampicin by using Eqs. 6–8 and 15–17. The values for IR were represented as an average and upper and lower limits when one S.D. for inter-individual variability of CYP3A4 baseline activity was considered.
doi:10.1371/journal.pone.0070330.t001

its degradation was negligible during the time period of the experiment. Even when the metabolism of rifampicin was incorporated into the *in vitro* CYP3A4 induction model using a reported generation rate of the metabolite [58], differences in parameter estimation were at most 16% (data not shown). A notable point of the analysis was that the parameter optimization procedure could be carried out directly without providing the $k_{cyp,deg}$ value. Because it was a parameter sensitive to the difference in the initial slope between the mRNA and activity profiles. In a conventional model which analyzes the activity profile alone, the maximally induced state needs to be presented in the profile to estimate the parameter. More interestingly, the $k_{cyp,deg}$ value estimated (0.0282 h^{-1}) was rather close to 0.03 h^{-1}, which was corrected for better *in vitro/in vivo* extrapolation [51,52], than a default k_{deg} value of the Simcyp simulator (0.0072 h^{-1}). It has been reported that the turnover half-lives for CYP3A4 determined by various methods ranged from 10 to 140 h [61], which corresponds to 0.005–0.07 h^{-1}. Although more information is needed to define an appropriate k_{deg}, the reasonable estimate was obtained from the *in vitro* data.

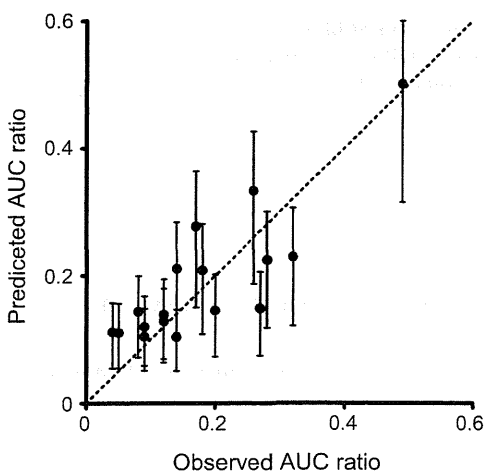

Figure 6. Correlation between predicted and observed *AUC* values for various drugs co-administered with rifampicin. This figure was produced using the values listed in Table 1. Error bars for predicted values represent the standard deviation from the inter-individual variability in baseline CYP3A4 activity. Not that this variability was estimated using extended least squares analysis of *in vitro* data.
doi:10.1371/journal.pone.0070330.g006

The reduction of *AUC* because of rifampicin-induced DDI was satisfactorily predicted from *in vitro* CYP3A4 induction data (Fig. 5). The predictive correlation coefficient of the present dynamic model (Q^2: 0.684) was slightly better than that of a conventionally used indirect effect model with the $k_{cyp,deg}$ of 0.0072 h^{-1} (Q^2: 0.499) or 0.03 h^{-1} (Q^2: 0.570). Since these models can deal with the dynamics of CYP3A4 induction, the IRs for each drug were calculated according to the dosage regimen. As shown in Fig. 5, however, the level of CYP3A4 activity becomes stable on day 6 or later. Since most of the clinical DDI evaluations were carried out on these days (i.e. after 5 or more days of treatment with rifampicin), even a static model could also describe DDI (Q^2: 0.604). The advantage of dynamic models is that it allows the simulation of DDI even at the early stages of treatment. The present dynamic DDI model, which considers the induction of

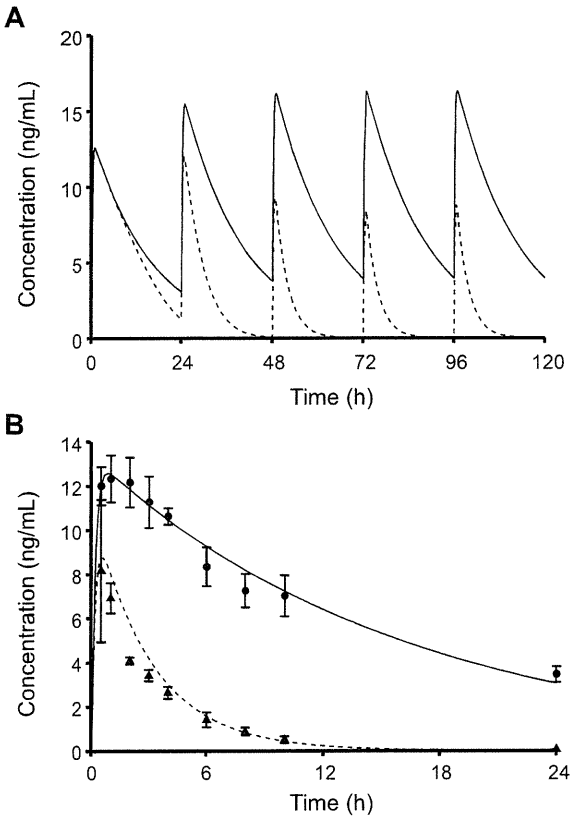

Figure 7. Simulation of DDI between alprazolam and rifampicin using a PHML/SBML hybrid model. Fig. 7A represents blood concentration profiles of repeated oral doses of alprazolam in the absence (solid line) and presence (broken line) of rifampicin. Fig. 7B represents the comparison between the predicted blood concentration of alprazolam with the corresponding clinical data (Ref. 35). Keys: 1 mg alprazolam alone (●, solid line); 1 mg alprazolam with 4-day pretreatment with daily doses of 450 mg rifampicin (▲, broken line). The pharmacokinetic parameters for alprazolam were estimated by curve-fitting to the blood concentrations following the sole administration (standard deviation of residuals, *RSD*: 0.483), and then used for predicting those following the concomitant administration (standard deviation of prediction errors, *SDEP*: 0.760). Both *RSD* and *SDEP* was the same in terms of formula: RSD or $SDEP = \sqrt{\sum (\text{experimental} - calculated)^2} \Big/ n$.
doi:10.1371/journal.pone.0070330.g007

CYP at not only the activity level but also at the mRNA level, was shown to successfully simulate the clearance time-course of alprazolam, a drug known to be metabolized by CYP3A4 (Fig. 7).

Rifampicin is known to induce other CYP enzymes moderately, as has also been described in the FDA guidance [62]. When rifampicin is concomitantly administered, clearance of bupropion (a CYP2B6 substrate), repaglinide (a CYP2C8 substrate), and warfarin (a CYP2C9 substrate) increases 2.1~3.4 times [63], 2.3 times [64], and 2.3~3.8 times [65,66], respectively. As compared with them, clearance of typical CYP3A4 substrates was much more induced (~10 times) (Table 1). A review article [67] compiled information on DDI with rifampicin and indicated that rifampicin induces CYP3A4 more efficiently than other CYPs, glucuronosyltransferases (UGTs), and p-glycoprotein. Taking them into account, induction of other enzymes than CYP3A4 would minimally affect the results of prediction, unless the fm_{CYP3A4} of substrates was extremely low. Gefitinib (fm_{CYP3A4}: 0.39) is known to be metabolized largely by CYP2D6 [68], which is little induced by rifampicin. On the other hand, imatinib (fm_{CYP3A4}: 0.28) is metabolized by CYP2C8 to the similar extent with CYP3A4 [69], resulting in slightly possible underestimation of DDI due to rifampicin. Prednisolone (fm_{CYP3A4}: 0.18) has been reported not to be metabolized by any other CYPs than CYP3A4 or UGTs [70]. Although the reasons why the fm_{CYP3A4} of prednisolone is low remain unclear, the fm_{CYP3A4} of 0.18 gave a good prediction of the DDI due to rifampicin. As long as the results were viewed as fair, induction of other enzymes or transporters might not be important in determining DDI between CYP3A substrates and rifampicin.

PHML, which inherited *insilico*ML (ISML) [71], is a new XML-based specification to describe a wide variety of models of biological and physiological functions with hierarchical structures. It can describe mathematical models consisting of ordinary differential equations, partial differential equations, agent-based simulation models, and others. In a similar way to ISML [71], a model is described by a set of functional elements (modules), each of which specifies mathematical expressions of the module functions. PhysioDesigner acts as a graphical editor and browser of the models written in PHML or ISML. A notable feature of PhysioDesigner is that it provides a function for creating SBML-PHML hybrid models. Since SBML is widely distributed as a standard format for representing and sharing models of biochemical reaction networks, it enables us to create multi-level physiological model systems. The functions of PhysioDesigner allowed us to dynamically connect PBPK-based DDI models with an enzyme transcription/translation dynamics model. Since the module-based hybrid model is highly reusable, extension to more comprehensive network models would be expected in future.

Supporting Information

Figure S1 Simulation of blood concentration of CYP3A4 substrate drugs following their oral administration. Keys: sole administration (●, solid line); 5-day pretreatment with daily doses with 600 mg rifampicin (▲, dash line). Pharmacokinetic parameters for each drug were estimated by curve-fitting to the blood concentrations following the sole administration, and then used for predicting those following co-administration with rifampicin. The pharmacokinetic parameters are given in Table S2.
(DOC)

Table S1 Pharmacokinetic data for CYP3A4 substrates.
(DOC)

Table S2 Pharmacokinetic parameters of CYP3A4 substrates.
(DOC)

Author Contributions

Conceived and designed the experiments: FY HS. Performed the experiments: YS SY AH MH. Analyzed the data: FY. Wrote the paper: FY. Developed the model used in simulation: FY HS. Developed the software used in analysis: YA HK.

References

1. Honig PK, Wortham DC, Zamani K, Conner DP, Mullin JC, et al. (1993) Terfenadine-ketoconazole interaction. Pharmacokinetic and electrocardiographic consequences. JAMA 269: 1513–1518.
2. Josephson F (2010) Drug-drug interactions in the treatment of HIV infection: focus on pharmacokinetic enhancement through CYP3A inhibition. J Intern Med 268: 530–539.
3. Grub S, Bryson H, Goggin T, Lüdin E, Jorga K (2001) The interaction of saquinavir (soft gelatin capsule) with ketoconazole, erythromycin and rifampicin: comparison of the effect in healthy volunteers and in HIV-infected patients. Eur J Clin Pharmacol 57: 115–121.
4. Capone D, Aiello C, Santoro GA, Gentile A, Stanziale P, et al. (1996) Drug interaction between cyclosporine and two antimicrobial agents, josamycin and rifampicin, in organ-transplanted patients. Int J Clin Pharmacol Res 16: 73–76.
5. Lattes R, Radisic M, Rial M, Argento J, Casadei D (1999) Tuberculosis in renal transplant recipients. Transpl Infect Dis 1: 98–104.
6. Modry DL, Stinson EB, Oyer PE, Jamieson SW, Baldwin JC, et al. (1985) Acute rejection and massive cyclosporine requirements in heart transplant recipients treated with rifampin. Transplantation 39: 313–314.
7. Kato M, Shitara Y, Sato H, Yoshisue K, Hirano M, et al. (2008) The quantitative prediction of CYP-mediated drug interaction by physiologically based pharmacokinetic modeling. Pharm Res 25: 1891–1901.
8. Galetin A, Burt H, Gibbons L, Houston JB (2006) Prediction of time-dependent CYP3A4 drug-drug interactions: impact of enzyme degradation, parallel elimination pathways, and intestinal inhibition. Drug Metab Dispos 34: 166–175.
9. Kanamitsu S, Ito K, Sugiyama Y (2000) Quantitative prediction of in vivo drug-drug interactions from in vitro data based on physiological pharmacokinetics: use of maximum unbound concentration of inhibitor at the inlet to the liver. Pharm Res 17: 336–343.
10. Ito K, Brown HS, Houston JB (2004) Database analyses for the prediction of in vivo drug-drug interactions from in vitro data. Br J Clin Pharmacol 57: 473–486.
11. Kato M, Chiba K, Horikawa M, Sugiyama Y (2005) The quantitative prediction of in vivo enzyme-induction caused by drug exposure from in vitro information on human hepatocytes. Drug Metab Pharmacokinet 20: 236–243.
12. Shou M, Hayashi M, Pan Y, Xu Y, Morrissey K, et al. (2008) Modeling, prediction, and in vitro in vivo correlation of CYP3A4 induction. Drug Metab Dispos 36: 2355–2370.
13. Almond LM, Yang J, Jamei M, Tucker GT, Rostami-Hodjegan A (2009) Towards a quantitative framework for the prediction of DDIs arising from cytochrome P450 induction. Curr Drug Metab 10: 420–432.
14. Grime K, Ferguson DD, Riley RJ (2010) The use of HepaRG and human hepatocyte data in predicting CYP induction drug-drug interactions via static equation and dynamic mechanistic modelling approaches. Curr Drug Metab 11: 870–885.
15. Yang J, Liao M, Shou M, Jamei M, Yeo KR, et al. (2008) Cytochrome p450 turnover: regulation of synthesis and degradation, methods for determining rates, and implications for the prediction of drug interactions. Curr Drug Metab 9: 384–394.
16. Fahmi OA, Hurst S, Plowchalk D, Cook J, Guo F, et al. (2009) Comparison of different algorithms for predicting clinical drug-drug interactions, based on the use of CYP3A4 in vitro data: predictions of compounds as precipitants of interaction. Drug Metab Dispos 37: 1658–1666.
17. Zhang JG, Ho T, Callendrello AL, Crespi CL, Stresser DM (2010) A multi-endpoint evaluation of cytochrome P450 1A2, 2B6 and 3A4 induction response in human hepatocyte cultures after treatment with β-naphthoflavone, phenobarbital and rifampicin. Drug Metab Lett 4: 185–194.
18. Pascussi JM, Robert A, Nguyen M, Walrant-Debray O, Garabedian M, et al. (2005) Possible involvement of pregnane X receptor-enhanced CYP24 expression in drug-induced osteomalacia. J Clin Invest 115: 177–186.
19. Parkinson A, Mudra DR, Johnson C, Dwyer A, Carroll KM (2004) The effects of gender, age, ethnicity, and liver cirrhosis on cytochrome P450 enzyme activity in human liver microsomes and inducibility in cultured human hepatocytes. Toxicol Appl Pharmacol 199: 193–209.
20. LeCluyse E, Madan A, Hamilton G, Carroll K, DeHaan R, et al. (2000) Expression and regulation of cytochrome P450 enzymes in primary cultures of human hepatocytes. J Biochem Mol Toxicol 14: 177–188.
21. Sheiner LB, Grasela TH (1984) Experience with NONMEM: analysis of routine phenytoin clinical pharmacokinetic data. Drug Metab Rev 15: 293–303.
22. Sheiner LB, Beal SL (1985) Pharmacokinetic parameter estimates from several least squares procedures: superiority of extended least squares. J Pharmacokinet Biopharm 13: 185–201.
23. Ohno Y, Hisaka A, Suzuki H (2007) General framework for the quantitative prediction of CYP3A4-mediated oral drug interactions based on the AUC increase by coadministration of standard drugs. Clin Pharmacokinet 46: 681–696.
24. Ohno Y, Hisaka A, Ueno M, Suzuki H (2008) General framework for the prediction of oral drug interactions caused by CYP3A4 induction from in vivo information. Clin Pharmacokinet 47: 669–680.
25. Backman JT, Luurila H, Neuvonen M, Neuvonen PJ (2005) Rifampin markedly decreases and gemfibrozil increases the plasma concentrations of atorvastatin and its metabolites. Clin Pharmacol Ther 78: 154–167.
26. Bolton AE, Peng B, Hubert M, Krebs-Brown A, Capdeville R, et al. (2004) Effect of rifampicin on the pharmacokinetics of imatinib mesylate (Gleevec, STI571) in healthy subjects. Cancer Chemother Pharmacol 53: 102–106.
27. Chung E, Nafziger AN, Kazierad DJ, Bertino JS (2006) Comparison of midazolam and simvastatin as cytochrome P450 3A probes. Clin Pharmacol Ther 79: 350–361.
28. Kivistö KT, Lamberg TS, Neuvonen PJ (1999) Interactions of buspirone with itraconazole and rifampicin: effects on the pharmacokinetics of the active 1-(2-pyrimidinyl)-piperazine metabolite of buspirone. Pharmacol Toxicol 84: 94–97.
29. Kyrklund C, Backman JT, Kivistö KT, Neuvonen M, Laitila J, et al. (2000) Rifampin greatly reduces plasma simvastatin and simvastatin acid concentrations. Clin Pharmacol Ther 68: 592–597.
30. McAllister WA, Thompson PJ, Al-Habet SM, Rogers HJ (1983) Rifampicin reduces effectiveness and bioavailability of prednisolone. Br Med J (Clin Res Ed) 286: 923–925.
31. Swaisland HC, Ranson M, Smith RP, Leadbetter J, Laight A, et al. (2005) Pharmacokinetic drug interactions of gefitinib with rifampicin, itraconazole and metoprolol. Clin Pharmacokinet 44: 1067–1081.
32. Villikka K, Kivistö KT, Lamberg TS, Kantola T, Neuvonen PJ (1997) Concentrations and effects of zopiclone are greatly reduced by rifampicin. Br J Clin Pharmacol 43: 471–474.
33. Villikka K, Kivistö KT, Luurila H, Neuvonen PJ (1997) Rifampin reduces plasma concentrations and effects of zolpidem. Clin Pharmacol Ther 62: 629-634.
34. Villikka K, Kivistö KT, Backman JT, Olkkola KT, Neuvonen PJ (1997) Triazolam is ineffective in patients taking rifampin. Clin Pharmacol Ther 61: 8–14.
35. Schmider J, Brockmöller J, Arold G, Bauer S, Roots I (1999) Simultaneous assessment of CYP3A4 and CYP1A2 activity in vivo with alprazolam and caffeine. Pharmacogenetics 9: 725–734.
36. Hebert MF, Roberts JP, Prueksaritanont T, Benet LZ (1992) Bioavailability of cyclosporine with concomitant rifampin administration is markedly less than predicted by hepatic enzyme induction. Clin Pharmacol Ther 52: 453–457.
37. Holtbecker N, Fromm MF, Kroemer HK, Ohnhaus EE, Heidemann H (1996) The nifedipine-rifampin interaction. Evidence for induction of gut wall metabolism. Drug Metab Dispos 24: 1121–1123.
38. Ridtitid W, Wongnawa M, Mahatthanatrakul W, Chaipol P, Sunbhanich M (2000) Effect of rifampin on plasma concentrations of mefloquine in healthy volunteers. J Pharm Pharmacol 52: 1265–1269.
39. Shi J, Montay G, Bhargava VO (2005) Clinical pharmacokinetics of telithromycin, the first ketolide antibacterial. Clin Pharmacokinet 44: 915–934.
40. Backman JT, Olkkola KT, Neuvonen PJ (1996) Rifampin drastically reduces plasma concentrations and effects of oral midazolam. Clin Pharmacol Ther 59: 7–13.
41. Acocella G, Pagani V, Marchetti M, Baroni GC, Nicolis FB (1971) Kinetic studies on rifampicin. I. Serum concentration analysis in subjects treated with different oral doses over a period of two weeks. Chemotherapy 16: 356–370.
42. Garcia M, Rager J, Wang Q, Strab R, Hidalgo IJ, et al. (2003) Cryopreserved human hepatocytes as alternative in vitro model for cytochrome p450 induction studies. In Vitro Cell Dev Biol Anim 39: 283–287.
43. Hariparsad N, Nallani SC, Sane RS, Buckley DJ, Buckley AR, et al. (2004) Induction of CYP3A4 by efavirenz in primary human hepatocytes: comparison with rifampin and phenobarbital. J Clin Pharmacol 44: 1273–1281.
44. Hariparsad N, Carr BA, Evers R, Chu X (2008) Comparison of immortalized Fa2N-4 cells and human hepatocytes as in vitro models for cytochrome P450 induction. Drug Metab Dispos 36: 1046–1055.
45. Li AP, Jurima-Romet M (1997) Applications of primary human hepatocytes in the evaluation of pharmacokinetic drug-drug interactions: evaluation of model drugs terfenadine and rifampin. Cell Biol Toxicol 13: 365–374.
46. Prueksaritanont T, Richards KM, Qiu Y, Strong-Basalyga K, Miller A, et al. (2005) Comparative effects of fibrates on drug metabolizing enzymes in human hepatocytes. Pharm Res 22: 71–78.
47. Acocella G (1978) Clinical pharmacokinetics of rifampicin. Clin Pharmacokinet 3: 108–127.
48. Hucka M, Finney A, Sauro HM, Bolouri H, Doyle JC, et al. (2003) The systems biology markup language (SBML): a medium for representation and exchange of biochemical network models. Bioinformatics 19: 524–531.
49. Ghosh S, Matsuoka Y, Asai Y, Hsin KY, Kitano H (2011) Software for systems biology: from tools to integrated platforms. Nat Rev Genet 12: 821–832.
50. Kitano H, Funahashi A, Matsuoka Y, Oda K (2005) Using process diagrams for the graphical representation of biological networks. Nat Biotechnol 23: 961–966.
51. Wang YH (2010) Confidence assessment of the Simcyp time-based approach and a static mathematical model in predicting clinical drug-drug interactions for mechanism-based CYP3A inhibitors. Drug Metab Dispos 38: 1094–1104.
52. Friedman EJ, Fraser IP, Wang YH, Bergman AJ, Li CC, et al. (2011) Effect of different durations and formulations of diltiazem on the single-dose pharmacokinetics of midazolam: how long do we go? J Clin Pharmacol 51: 1561–1570.
53. Ourlin JC, Lasserre F, Pineau T, Fabre JM, Sa-Cunha A, et al. (2003) The small heterodimer partner interacts with the pregnane X receptor and represses its transcriptional activity. Mol Endocrinol 17: 1693–1703.

54. Li T, Chiang JY (2006) Rifampicin induction of CYP3A4 requires pregnane X receptor cross talk with hepatocyte nuclear factor 4alpha and coactivators, and suppression of small heterodimer partner gene expression. Drug Metab Dispos 34: 756–764.
55. Yang J, Yan B (2007) Photochemotherapeutic agent 8-methoxypsoralen induces cytochrome P450 3A4 and carboxylesterase HCE2: evidence on an involvement of the pregnane X receptor. Toxicol Sci 95: 13–22.
56. Xie W, Yeuh MF, Radominska-Pandya A, Saini SP, Negishi Y, et al. (2003) Control of steroid, heme, and carcinogen metabolism by nuclear pregnane X receptor and constitutive androstane receptor. Proc Natl Acad Sci U S A 100: 4150–4155.
57. Chen Y, Ferguson SS, Negishi M, Goldstein JA (2004) Induction of human CYP2C9 by rifampicin, hyperforin, and phenobarbital is mediated by the pregnane X receptor. J Pharmacol Exp Ther 308: 495–501.
58. Nakajima A, Fukami T, Kobayashi Y, Watanabe A, Nakajima M, et al. (2011) Human arylacetamide deacetylase is responsible for deacetylation of rifamycins: rifampicin, rifabutin, and rifapentine. Biochem Pharmacol 82: 1747–1756.
59. Furesz S, Scotti R, Pallanza R, Mapelli E (1967) Rifampicin: a new rifamycin. 3. Absorption, distribution, and elimination in man. Arzneimittelforschung 17: 534–537.
60. Poulin P, Theil FP (2002) Prediction of pharmacokinetics prior to in vivo studies. 1. Mechanism-based prediction of volume of distribution. J Pharm Sci 91: 129–156.
61. Yang J, Liao M, Shou M, Jamei M, Yeo KR, et al. (2008) Cytochrome P450 turnover: regulation of synthesis and degradation, methods for determining rates, and implications for the prediction of drug interactions. Curr Drug Metab 9: 384–393.
62. Guidance for industry. drug interaction studies – study design, data analysis, implications for dosing, and labeling recommendations. Available: http://www.fda.gov/downloads/Drugs/GuidanceComplianceRegulatoryInformation/Guidances/ucm292362.pdf.
63. Chung JY, Cho JY, Lim HS, Kim JR, Yu KS, et al. (2011) Effects of pregnane X receptor (NR1I2) and CYP2B6 genetic polymorphisms on the induction of bupropion hydroxylation by rifampin. Drug Metab Dispos 39: 92–97.
64. Niemi M, Backman JT, Neuvonen M, Neuvonen PJ, Kivistö KT (2000) Rifampin decreases the plasma concentrations and effects of repaglinide. Clin Pharmacol Ther 68: 495–500.
65. O'Reilly RA (1974) Interaction of sodium warfarin and rifampicin. studies in man. Ann Intern Med 81: 337–340.
66. Heimark LD, Gibaldi M, Trager WF, O'Reilly RA, Goulart DA (1987) The mechanism of the warfarin-rifampin drug interaction in humans. Clin Pharmacol Ther 42:388–394.
67. Chen J, Raymond K (2006) Roles of rifampicin in drug-drug interactions: underlying molecular mechanisms involving the nuclear pregnane X receptor. Ann Clin Microb Antimicrob 5: 3.
68. Li J, Zhao M, He P, Hidalgo M, Baker SD (2007) Differential metabolism of gefitinib and erlotinib by human cytochrome P450 enzymes. Clin Cancer Res 13: 3731–3737.
69. Nebot N, Crettol S, d'Esposito F, Tattam B, Hibbs DE, et al. (2010) Participation of CYP2C8 and CYP3A4 in the N-demethylation of imatinib in human hepatic microsomes. Br J Pharmacol 161: 1059–1069.
70. Zhang ZY, Chen M, Chen J, Padval MV, Kansra VV (2009) Biotransformation and in vitro assessment of metabolism-associated drug–drug interaction for CRx-102, a novel combination drug candidate. J Pharm Biomed Anal 50: 200–209.
71. Asai Y, Suzuki Y, Kido Y, Oka H, Heien E, et al. (2008) Specifications of insilicoML 1.0: a multilevel biophysical model description language. J Physiol Sci 58: 447–458.

Mol Neurobiol (2014) 49:88–102
DOI 10.1007/s12035-013-8489-4

Integrating Pathways of Parkinson's Disease in a Molecular Interaction Map

Kazuhiro A. Fujita · Marek Ostaszewski · Yukiko Matsuoka · Samik Ghosh · Enrico Glaab · Christophe Trefois · Isaac Crespo · Thanneer M. Perumal · Wiktor Jurkowski · Paul M. A. Antony · Nico Diederich · Manuel Buttini · Akihiko Kodama · Venkata P. Satagopam · Serge Eifes · Antonio del Sol · Reinhard Schneider · Hiroaki Kitano · Rudi Balling

Received: 15 April 2013 / Accepted: 13 June 2013 / Published online: 7 July 2013

Abstract Parkinson's disease (PD) is a major neurodegenerative chronic disease, most likely caused by a complex interplay of genetic and environmental factors. Information on various aspects of PD pathogenesis is rapidly increasing and needs to be efficiently organized, so that the resulting data is available for exploration and analysis. Here we introduce a computationally tractable, comprehensive molecular interaction map of PD. This map integrates pathways implicated in PD pathogenesis such as synaptic and mitochondrial dysfunction, impaired protein degradation, alpha-synuclein pathobiology and neuroinflammation. We also present bioinformatics tools for the analysis, enrichment and annotation of the map, allowing the research community to open new avenues in PD research. The PD map is accessible at http://minerva.uni.lu/pd_map.

Keywords Parkinson's disease · Molecular neuropathology · Knowledge repository · Bioinformatics

K. Fujita and M. Ostaszewski contributed equally to this work.

Electronic supplementary material The online version of this article (doi:10.1007/s12035-013-8489-4) contains supplementary material, which is available to authorized users.

Introduction

Parkinson's disease (PD) is a major neurodegenerative disease, characterized clinically by a range of symptoms, in particular, impaired motor behaviour. The pathogenesis of PD is multi-factorial and age-related, implicating various genetic and environmental factors [1]. Gaps in the understanding of the underlying molecular mechanisms hamper the design of effective disease modifying therapies. Investigation of such a complex disease requires a proper knowledge repository that

K. A. Fujita · Y. Matsuoka · S. Ghosh · H. Kitano
The Systems Biology Institute, Minato-ku, Tokyo, Japan

M. Ostaszewski · E. Glaab · C. Trefois · I. Crespo · T. M. Perumal · W. Jurkowski · P. M. A. Antony · N. Diederich · M. Buttini · V. P. Satagopam · S. Eifes · A. del Sol · R. Schneider · R. Balling (✉)
Luxembourg Centre for Systems Biomedicine (LCSB), University of Luxembourg, 7, Avenue des Hauts-Fourneaux, Esch-sur-Alzette, Luxembourg
e-mail: rudi.balling@uni.lu

M. Ostaszewski
Integrated Biobank of Luxembourg, Luxembourg City, Luxembourg

N. Diederich
Department of Neuroscience, Centre Hospitalier Luxembourg, Luxembourg City, Luxembourg

A. Kodama
Faculty of Medicine, Tokyo Medical and Dental University, Tokyo, Japan

V. P. Satagopam · R. Schneider
Computational Biology Unit, European Molecular Biology Laboratory, Heidelberg, Germany

H. Kitano
Sony Computer Science Laboratories, Shinagawa-ku, Tokyo, Japan

H. Kitano
Division of Systems Biology, Cancer Institute, Tokyo, Japan

H. Kitano
Open Biology Unit, Okinawa Institute of Science and Technology, Kunigami, Okinawa, Japan

organizes the rapidly growing PD-related knowledge — a disease map.

The concept of a disease map is relatively new and has found only a limited application in the field of neurodegenerative diseases thus far [2, 3]. Such a map represents diagrammatically interactions between molecular components and pathways reported to play a role in disease pathogenesis and progression. It provides navigation and exploration tools that help the user to locate specific areas of interest and visualize known interactions. Associated analytical tools allow investigators to develop a profound understanding of the disease, detect unexpected interactions and ultimately identify new research hypotheses.

In this paper, we present a PD molecular interaction map that captures and visualizes all major molecular pathways involved in PD pathogenesis. Furthermore, it constitutes a resource for computational analyses and a platform for community level collaborations [4, 5] (see Fig. 1). We also present how a set of bioinformatics tools applied to the map can facilitate in-depth knowledge extraction and continuous curation.

The paper is divided into two parts. In the first part, we review the pathways implicated in PD, with a focus on synaptic and mitochondrial dysfunction, α-synuclein pathobiology, failure of protein degradation systems, neuroinflammation and apoptosis. In the second part of the paper, we demonstrate how the PD map interfaces with bioinformatics tools and databases for its content annotation, enrichment with experimental results, and analysis of its complex structure and dynamics. The PD map is accessible under http://minerva.uni.lu/pd_map (Online resource 1), as a SBML file (Online resource 2), and Payao, a community platform for pathway model curation [264].

Neurodegeneration in Parkinson's Disease Arises from Dysregulation of Interlinked Molecular Pathways

The major pathological feature of PD is the progressive degeneration of the nigrostriatal system, leading to the loss of dopaminergic (DA) neurons in the substantia nigra pars compacta (SNpc) [6]. The degeneration of the nigrostriatal pathway and subsequent loss of striatal dopamine contributes to the cardinal clinical motor symptoms: tremor, rigidity, bradykinesia and postural instability [7]. Although treatments such as dopamine substitution and deep brain stimulation alleviate many of the motor symptoms, there is no disease-modifying therapy preventing the progressive loss of DA neurons [8].

Susceptibility for PD is modulated by various environmental factors [9–13], genetic predisposition or risk factors [14] and epigenetic alterations [15, 16].[1] Exposure to pesticides and industrial agents has been associated with an increased risk for PD [17, 18], but to date none of these agents have been consistently identified as a causal factor for PD [19]. It is known that exposure to inhibitors of mitochondrial respiration [20–25] are sufficient to induce PD symptoms in humans and DA neurodegeneration in animal models.

In this paper, we focus on DA neurons as a major point of convergence in PD disease pathways. However, pathogenic pathways leading to the demise of DA neurons may impact any neuronal population affected in PD, including those of the autonomic ganglia [26, 27]. The demise of these populations may contribute to a range of PD-typical non-motor symptoms hampering the life of PD patients, such as constipation and dysautonomia (ganglia of autonomous nervous system), cognitive decline and REM sleep behaviour (cholinergic neurons of the nucleus basalis of Meynert, noradrenergic coeruleus–subcoeruleus complex), depression and apathy (serotinergic caudal raphe nuclei, cholinergic gigantocellular reticular nucleus) [28, 29].

Vulnerability and Preferential Loss of Midbrain Dopaminergic Neurons

SNpc DA neurons are the most vulnerable population of neurons in PD. It has been suggested that their loss is multifactorial and related to the characteristic features of these cells: complex morphology, high energy demand, high calcium flux, and dopamine metabolism [30]. Consequently, these neurons are particularly susceptible to various stressors, which contribute to their preferential loss (see Fig. 2).

SNpc DA neurons have one of the longest yet most dense arborisation of all neurons [31, 32]. They project to the striatum, providing it with DA [33, 34]. These neurons have long, thin, mostly unmyelineated axons [35] and up to 150,000 presynaptic terminals per neuron [30]. The high energy demand required to support synaptic activity, compensation for the potential risk of depolarization in the unmyelinated membrane, and axonal transport over long distances put a huge burden on the mitochondria. Interestingly, toxins that perturb the energy production and the axonal transport of mitochondria [36], cause parkinsonism in humans and preferential loss of DA neurons in animal models [22, 36, 37]. Finally, the large number of synapses increases the risk for local α-synuclein (α-syn) misfolding (see sections "Synaptic Dysfunction" and "α-Synuclein Misfolding and Pathobiology").

SNpc DA neurons can fire autonomously and have specific calcium L-type Cav 1.3 channels that regulate this pacemaking activity [38, 39]. The resulting high intracytosolic Ca^{2+} concentrations induce cellular stress, elevate the levels of reactive oxygen species (ROS), and increase demand for calcium buffering, which is handled by the endoplasmic reticulum (ER) and the mitochondria. Maintaining proper calcium homeostasis in such an environment increases again the

[1] Epigenetic alterations — secondary, environmentally induced changes of gene expression.

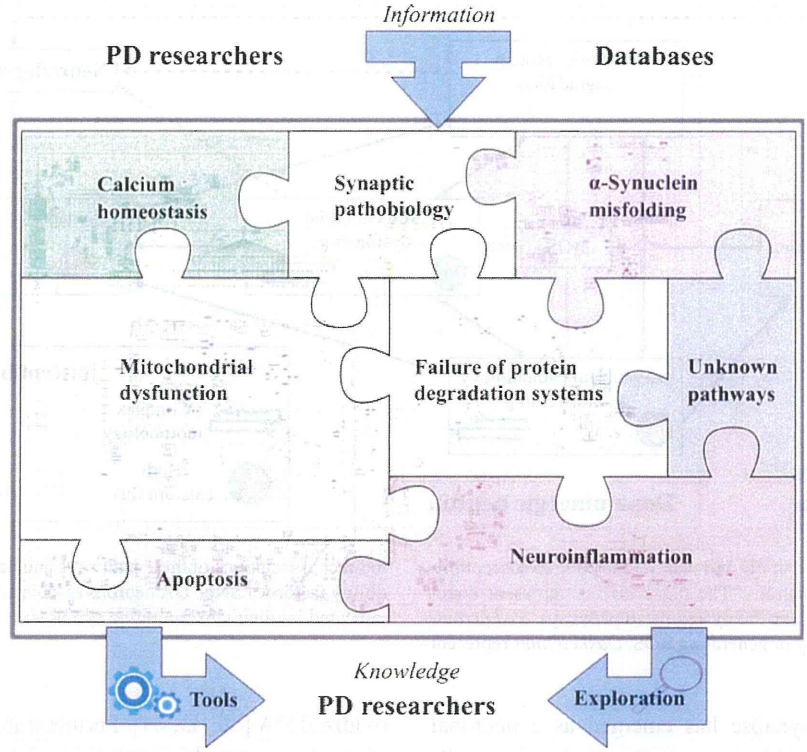

Fig. 1 The concept of Parkinson's disease map and its possibilities. The PD map is a knowledge repository bringing together different molecular mechanisms and pathways considered to be the key players in the disease. The current focus of the map is illustrated by the pieces in the "PD puzzle" These modules include synaptic and mitochondrial dysfunction, failure of protein degradation systems, α-synuclein pathobiology and misfolding, and neuroinflammation. Processes important in PD-associated neurodegeneration, such calcium homeostasis or apoptosis, are discussed within their appropriate context in the main text, and included into the PD map pathways. The PD map is represented as a graph constructed with all gene-regulatory protein and metabolic interactions extracted from published data. Currently the map has 2,285 elements and 989 reactions supported by 429 articles and 254 entries from publicly available bioinformatic databases. It is compliant with standardized graphical representation, Systems Biology Graphical Notation (*SBGN*) [265]. This standardized representation of the map could become a common language for the PD research community to discuss disease-related molecular mechanisms [5]. Detailed contents of the PD map are accessible at http://minerva.uni.lu/MapViewer/map?id=pdmap (Online resource 1) as an SBML file (Online resource 2) and in Payao [264]. The map can be updated with information from the PD research community, as well as by searching bioinformatics databases. Exploration and analysis of the content has the potential to broaden knowledge on the molecular processes in PD, generate of new hypotheses on disease pathogenesis, or prioritize the most interesting areas and molecules for investigation. Approaches to facilitate this knowledge acquisition process are discussed in detail in the section "Annotation, enrichment and Analysis of the PD Map"

energy needs. In contrast, neighbouring dopamine neurons in the ventral tegmental area use Na^+ channels for pacemaking and are relatively spared in PD [37].

Cytosolic DA also contributes to the vulnerability of DA neurons, primarily because its metabolism induces oxidative and nitrative stress in an age-dependent manner [40–42]. Neurotoxicity of DA increases with its concentration, which is thought to be regulated by Ca^{2+} concentration [43]. Additionally, dopamine metabolism is involved in a number of PD-associated pathways, as it can impair synapse function, inhibit protein degradation and disturb mitochondrial dynamics by inhibiting the function of Parkin.

Ageing, the primary risk factor for PD, especially affects DA neurons (see Fig. 2). α-Syn accumulation increases with age in the SNpc and correlates with the loss of DA neurons in non-human primates [42]. This could be linked to the age-related impairment of the two protein degradation systems: the ubiquitin–proteasome system (UPS) [42] and the autophagy–lysosome system [44]. ROS accumulate in an ageing brain [42, 45], partially due to mitochondria dysfunction, as mitophagy[2] is decreased with ageing [45, 46]. Finally, the threshold required to trigger a neuroinflammatory response may decrease with age, since glial activation in SNpc increases in the ageing brain [42, 47].

Synaptic Dysfunction

The main function of a synapse is to establish a connection between neurons allowing communication via chemical or

[2] Mitophagy — autophagy of mitochondria.

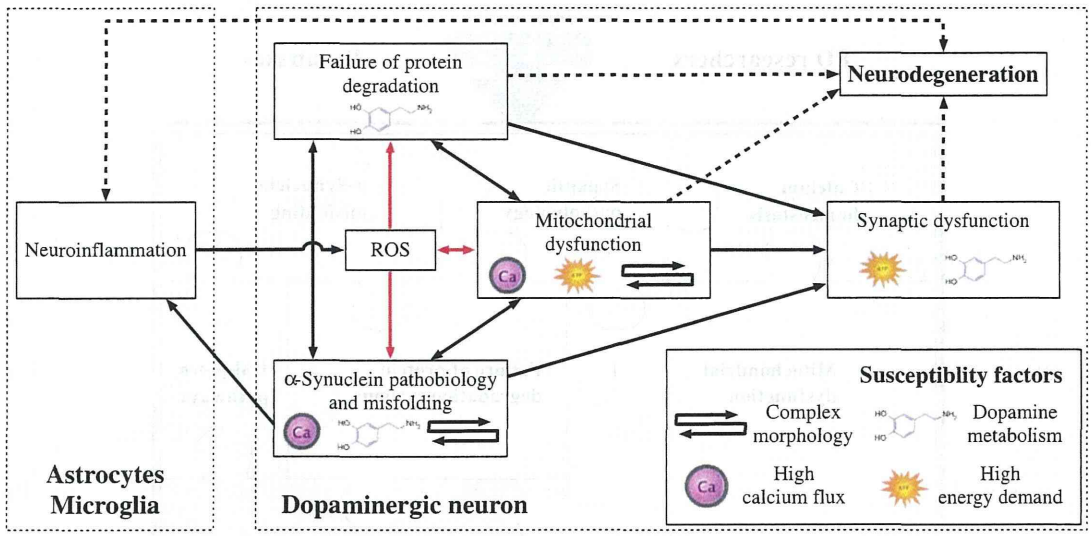

Fig. 2 Pathways implicated in PD and their relationship to susceptibility factors of SNpc DA neurons. The *black arrows* represent direct molecular interactions between the dysregulated pathways. *Red arrows* denote pathways affected by or generating ROS. *Dashed lines* represent indirect associations of these pathways and neurodegeneration. Susceptibility factors of SNpc DA neurons associated with a given pathway are indicated by their corresponding symbols

electric signals. The synapse has emerged as a neuronal structure highly susceptible to a variety of chronic insults [48–51]. Below, we discuss the increasing evidence indicating that synapses are also affected in PD, and that their dysfunction and demise contributes to the disease.

α-Syn is a presynaptic protein. Point mutations, duplications or triplications of its gene are associated with familial PD [52–54]. In cultured neurons, it transiently associates with synaptic vesicles prior to neurotransmitter release, upon which it rapidly redistributes to the cytosol [55]. Association of α-syn with the synaptic vesicle may occur through its binding to SNARE complex proteins [56], and, as shown in mice, α-syn positively influences functional SNARE levels [57]. Similarly, upregulation of α-syn in synapses and cell somas of cultured neurons protects against oxidative stress [58]. However, the protective effect of α-syn is limited to a narrow concentration range, since high levels of α-syn cause familial PD [53]. Even modest overexpression of α-syn has been reported to markedly inhibit neurotransmitter release [59]. Also, α-syn forms potentially pathogenic microaggregates in the synapse [60]. Another protein involved familial and sporadic PD, LRRK2, is also present in the synapse. Its experimentally induced upregulation or knockdown impairs the dynamics of synaptic vesicle release and recycling [61, 62]. However, the influence of mutated or dysfunctional LRRK2 on these processes in PD remains to be investigated.

A number of other PD-related pathological events might affect synapses. Synapses of the nigrostriatal pathway, with their high level of α-syn and dopamine, are likely to be the major site of the formation of toxic adducts of α-syn and oxidized DA [40, 63, 64]. Furthermore, the energy demands of synapses may be compromised by dysfunctional mitochondrial respiration, turnover, or axonal transport [65]. Locally dysfunctional protein degradation and turnover may directly affect synaptic function and plasticity [66].

Mitochondrial Dysfunction

Mitochondria are highly dynamic organelles essential for a range of cellular processes including ATP production, ROS management, calcium homeostasis, and control of apoptosis. The maintenance of mitochondrial homoeostasis by mitophagy involves multiple factors ranging from the control of mitochondrial fusion and fission to mitochondrial motility [67]. These processes are strongly related to proteins involved in familial and sporadic PD [65, 68, 69].

A number of proteins associated with familial PD are related to mitochondrial function [70], with PINK1 and Parkin playing a particularly important role. Control of mitochondrial turnover and protection against oxidative stress are mediated via the kinase activity of PINK1 targeting Parkin [71], HTRA2 [72] and TRAP1[73] proteins. In turn, mitophagy is driven by PINK1-mediated translocation of Parkin from the cytosol to mitochondria [71, 74]. Importantly, both mitophagy [75, 76] and transcriptional control of mitochondrial biogenesis [77–79] depend on the E3 ubiquitin ligase activity of Parkin.

Familial PD genes are also implicated in ROS production by mitochondria. Mitochondrial respiration and calcium balance are perturbed by PINK1 deficiency [80, 81]. The resulting reduced mitochondrial calcium capacity and increased ROS

could lower the threshold for mitochondrial outer membrane permeabilization (MOMP) and thereby increase the vulnerability for cell death [80]. Additional detrimental downstream effects of excessive ROS are mitochondrial DNA damage and inflammation [65, 82]. It has been suggested that DJ1 works in parallel to the PINK1–Parkin pathway to maintain mitochondrial function in the presence of an oxidative environment [83]. DJ1 was shown to interact with a mitochondrial protein mortalin, which maintains mitochondrial homeostasis and antagonizes oxidative stress injury [84]. Remarkably, Parkin overexpression has been demonstrated to prevent mitochondrial dysfunction caused by a mortalin knockdown [85].

Mitochondrial trafficking is necessary for proper energy supply. This process is particularly demanding in long axons of DA neurons. Recent findings suggest that mitochondrial transport may be affected in PD. Axonal transport of mitochondria along the microtubules is directly influenced by PINK1 through its supporting role in the kinesin motor complex [86]. Also, PINK1 and Parkin may play an important role in the process of quarantining the damaged mitochondria prior to their clearance [87]. However, the role of PINK1 in the dynamics of mitochondrial trafficking is not yet fully understood [88]. Mitochondrial trafficking may also be impaired by Parkin, α-syn, or LRRK2 as they modulate microtubule stability [89–92], or by formation of α-syn aggregates [93].

Finally, other proteins associated with familial PD have recently been linked to mitochondrial pathways. UCHL1-mediated cell death can be attenuated by mitochondrial protein HTRA2 [94], ATP13A2 regulates mitochondrial bioenergetics through macroautophagy [95], VPS35 mediates vesicle transport between mitochondria and peroxisomes [96], and EIF4G1 is involved in stress related protection of mitochondria [97].

Failure of Protein Degradation Systems

In long-lived post-mitotic cells, such as neurons, the degradation systems assuring the removal of damaged, dysfunctional cellular structures play a key role in cellular homeostasis. These degradation systems are involved in the clearance of defective cellular structures such as misfolded or damaged proteins, and dysfunctional organelles such as defective mitochondria [98]. The two major degradation systems are the UPS and the autophagy–lysosome system. The complex machinery and biology of these two systems have been extensively reviewed elsewhere [66, 99–101]. The dysfunction of clearance systems, especially in the synapse, can lead to the accumulation of α-syn and defective mitochondria. These, in turn, can interfere with proper synaptic function, lead to the formation of toxic assemblies or aggregates, or impair energy metabolism and cause oxidative stress.

Genetic and pathological evidence strongly indicate the involvement of defective clearance systems in PD [102–104]. Interestingly, patients with Gaucher's disease, a lysosomal storage disorder [105, 106], have an increased risk for PD and accumulate α-syn in their brains [107]. Mutated forms of α-syn have been reported to inhibit their own degradation by chaperone-mediated autophagy (CMA), while DA-modified α-syn also blocks CMA degradation of other proteins [103]. Finally, pathological observations in PD autopsy brains and brains of PD animal models show an increased number of autophagy vacuoles and other autophagy markers [108, 109]. Interestingly, neurons containing Lewy bodies (LB) were shown to have decreased UPS and lysosomal markers [110].

While this evidence demonstrates the involvement of cellular clearance mechanisms in PD, it is unclear whether that involvement is primarily beneficial or detrimental. It has been argued that exaggerated clearance activity may contribute to neuronal injury [111, 112]. The predominant view, however, is that the removal of abnormal proteins and organelles is neuroprotective [102, 113–118].

α-Synuclein Misfolding and Pathobiology

The pathobiology of α-syn is implicated in a number of pathways involved in PD. α-Syn is an intrinsically disordered protein [119], which can spontaneously and dynamically adopt either physiological or misfolded conformations. The latter contains β-sheet structure, which promotes oligomerisation and fibrilisation [120–122]. High-order oligomeric and pre-fibrillar forms are thought to be cytotoxic, while fibrillar and aggregated forms may be harmless, detoxified depositions [119, 123]. This is still controversial, since familial PD α-syn mutants promote both misfolding and aggregation of α-syn, suggesting a pathological role of this process [103, 121, 124, 125].

Mutated, misfolded or overexpressed α-syn is involved in a number of pathways associated with degeneration of SNpc DA neurons. It is thought to impair synapse function [126–129] and to affect the respiration, morphology and turnover of mitochondria [130–134]. Axonal transport might be impaired by misfolded α-syn through perturbation of microtubule assembly [135–137], especially together with MAPT protein [138–143]. Also, oligomers of mutant α-syn induce chronic ER stress [125, 144], which seems to precede actual neurodegeneration [145]. Finally, α-syn degradation by CMA [146] might be perturbed by mutated or dopamine-modified α-syn [103, 146, 147]. Reduction of lysosomal activity by α-syn overexpression might lead to α-syn accumulation [148], suggesting a vicious loop of CMA deficiency and α-syn misfolding. The proteasome system has also been reported to be inhibited either by α-syn mutants [149–151], or oligomers [152].

Recent studies suggest that α-syn aggregates spread between cells and that this contributes to the PD disease process [123, 153]. This hypothesis is supported by reports of protein inclusions detected in previously unaffected DA neurons grafted into the striatum of PD patients [154–156]. The existence of a neuron-to-neuron transfer mechanism for misfolded α-syn has been shown in cell culture, primary mouse neurons and mouse models [157–159]. Moreover, it was observed that different types of cellular stress associated with PD pathogenesis, such as misfolded protein accumulation [160], proteasomal and mitochondrial dysfunction [161], are able to increase secretion of α-syn and its aggregates.

It has been shown that exogenous α-syn preformed fibrils might promote the aggregation of endogenous α-syn in neuronal cells [158, 159, 162] impairing neural function [158, 159]. Taken together, these results suggest that misfolded α-syn can be secreted and taken up, introducing additional cellular stress and promoting further protein misfolding.

Neuroinflammation

Neuroinflammation and chronic activation of the immune system are pathological processes associated with all chronic neurodegenerative diseases, such as PD, AD or multiple sclerosis [163]. Although the involvement of the adaptive immune system in PD-related neuroinflammation has been suggested [164, 165], in particular in the context of α-syn and neuromelanin [166, 167], current research of neuroinflammation in PD focuses primarily on the innate immune system. Of particular interest are microglia[3] [168] and astrocytes[4] [169, 170].

Microglia constantly explore and monitor the local environment [171, 172], modulating the response of the immune system in relation to the level of their perturbation. At the first sign of stress, they produce and release anti-inflammatory cytokines and supportive growth factors [168]. Neurons play an active role in regulating the microglial response. Many of their products inhibit microglia activation by binding to specific microglial receptors [173–177].

The SNpc is a brain region that may be especially vulnerable to elevated neuroinflammation. The SNpc contains more microglia [178] and less astrocytes than other brain regions [179]. With a high microglial density promoting the inflammatory response, and low astroglial density to downregulate it, neuroinflammation in the SNpc may be particularly strong. Moreover, SNpc neurons contain neuromelanin, which has been shown to activate microglia [180] and could be another factor promoting neuroinflammation.

[3] Microglia — the most abundant of the resident macrophage populations in the CNS.

[4] Astrocytes — glial cells that play a supportive role for neurons and modulate microglia response.

The response of glial cells in the context of PD has been studied in humans, animal models and cell cultures. The presence of reactive microglia in human post-mortem brain tissue has been reported in PD patients [181] and in people exposed to MPTP [182]. In animal models of PD, microglial activation has been studied in primates [183], mice [184] and rats [185], supporting the notion that neuroinflammation is intrinsically associated with the PD pathological process. In cellular co-cultures of neuronal cells and microglia, neuronal injury drives microglia activation, which in turn enhances neurodegeneration [186].

In vitro systems demonstrate that the delicate balance between protective and detrimental effects of glial response might be disrupted by PD-related stress factors. Microglia can detect misfolded α-syn [187, 188] and increase neurotoxicity by producing ROS and pro-inflammatory cytokines [189, 190]. In turn, activated microglia expressing LRRK2 with a PD-related mutation produce more pro-inflammatory cytokines than corresponding cells expressing WT LRRK2 [191]. Deficiency in Parkin may indirectly promote microglia activation by increasing neuronal vulnerability for inflammation-related stress [192] and disturbing the neuron–microglia balance. Finally, DJ-1 deficiency in astrocytes might contribute to neurodegeneration by deregulating their neuroinflammatory response [193].

In summary, many in vitro PD models indicate a detrimental role of microglia. However, the situation in vivo is less clear, even though protective effects of anti-inflammatory compounds such as minocycline have been reported in models of PD [194].

Neuronal Death Through Apoptosis-Related Mechanisms

Degeneration of DA neurons is the final consequence of dysregulated cellular processes, leading to neuronal death [195]. Neurodegeneration by apoptosis typically proceeds through one of two signalling cascades, termed the intrinsic and extrinsic pathways [196, 197].

The intrinsic pathway can be induced by intracellular stress, leading to MOMP that is controlled through proteins of the BCL-2 family. As a result, cytochrome *c* is released from the mitochondrial intermembrane space, leading to formation of an apoptosome and subsequent execution of apoptosis by activation of caspases 3 and 7. Studies in animal models of PD suggest the BCL-2 family is a key target for attenuating neurodegeneration of DA neurons [198–202].

Additionally, an important link between PD and the activation of apoptosis comes from studies investigating the roles of familial PD genes. It has been shown that disease-related LRRK2 mutations R1441C, Y1699C and G2019S promote mitochondria-dependent apoptosis [203]. PINK1 and Parkin, in turn, protect against stress-induced cytochrome

c release, while their mutations might fail to attenuate basal neuronal pro-apoptotic activity [204–206]. Importantly, failure of the protein degradation system could also contribute to apoptosis via the intrinsic pathway. It has been proposed that lysosome membrane permeabilization is induced by ROS and occurs upstream and downstream of MOMP [207, 208]. Finally, DA-mediated activation of the intrinsic pathway may contribute to selective DA neuron degeneration [209].

The extrinsic apoptosis pathway is activated by extracellular signalling, and diverges into two sub-pathways: one directly activating caspase 3 and 7, the other causing MOMP. Neuroinflammation could be a major factor in this process [165, 187, 210], promoting neuronal apoptosis either by oxidative insults [211] or by pro-inflammatory cytokines [212, 213].

In summary, both apoptosis pathways appear to be the convergence point of different pathways dysregulated in PD. Still, therapeutic interventions may be most efficacious in maintaining DA neuron functionality if aimed at the upstream events of apoptosis. Indeed, as the apoptotic process is advanced, the intervention may be too late.

Annotation, Enrichment and Analysis of the PD Map

Dysregulated pathways implicated in PD are strongly coupled, and their interconnections need to be represented in an integrated and comprehensive way to be studied efficiently. Our PD map allows navigation through information on PD-associated mechanisms, and constitutes an interface to well-established tools and methods for updating, enriching, and analysing its contents (see Fig. 3).

Annotation of the PD Map Using Bioinformatic Databases

We have enriched the elements of the PD map using a number of publicly available databases [214–230]. Information on official gene symbol, synonyms, description and chromosomal location; association with biological processes and diseases; or molecular interacting partners have been embedded within the map. Annotation of the contents of the PD map facilitates the knowledge exploration by providing additional information about map elements and their interactions, and is easily accessible online (see Fig. 3b for illustration and Online resource 1 for details).

Exploration of the Map Using Integrative Expression Analysis

Recently, a variety of PD-related large-scale datasets have become publicly available, including microarray gene expression data for human post mortem samples from different regions of the brain [231–234], human whole-blood samples [235], and samples from animal [236] and cell culture models [237]. This experimental data can be visualized on the PD map or used to predict new map elements and interactions [238–240].

Visualization of gene deregulation in PD-related microarray datasets [231–234] is possible via a variety of methods for candidate disease gene or protein prioritizations [241–244]. We have chosen an approach combining significance scores [245] for differentially expressed genes in multiple studies, and prepared a colour-coded version of the map highlighting upregulation in green and downregulation in red (see the online PD map and Online resource 1). This gives an immediate overview of pathways that are affected by dysregulated genes.

One of the major advantages of the PD map is the possibility to predict new elements and interactions on the basis of the map contents and experimental data. To achieve this, publicly available human molecular interaction data [242] are obtained for the PD map elements, extending the number of interactions. Then, an automated, graph-theoretic approach [243] prioritizes candidate disease proteins that are densely interconnected in the extended PD map, and whose gene expression levels are differentially expressed in the microarray PD samples. We have combined the abovementioned experimental microarray [231–234] and protein-protein interaction data [242] to demonstrate the usage of this approach. The extended PD map containing the prioritized new proteins can be found in Online resource 1.

PD Map as a Network: from Structural Analysis to Kinetic Models

The PD map is a large, complex network integrating metabolic reactions, gene regulation, and signalling processes. Exploring how different elements in the network may influence each other is difficult and non-intuitive. Graph-theoretical methods aim to bridge the gap between our understanding of the role of single elements in a cellular network and the properties of this network as whole [246, 247]. These methods aim to identify key network nodes (genes, proteins), edges (molecular interactions) or modules[5] (subnetworks) [246].

Basic properties of individual network elements such as node centrality[6] indicate their global role in the whole network. In turn, analysis of inter-modular communication[f] in

[5] Module — in the PD map by a module (subgraph, subnetwork) we understand elements and interactions participating in the same pathway or serve similar biological function. Inter-modular communication denotes all interactions linking different modules.

[6] Node centrality — a measure describing how important a given node is for the connectivity of the entire network.

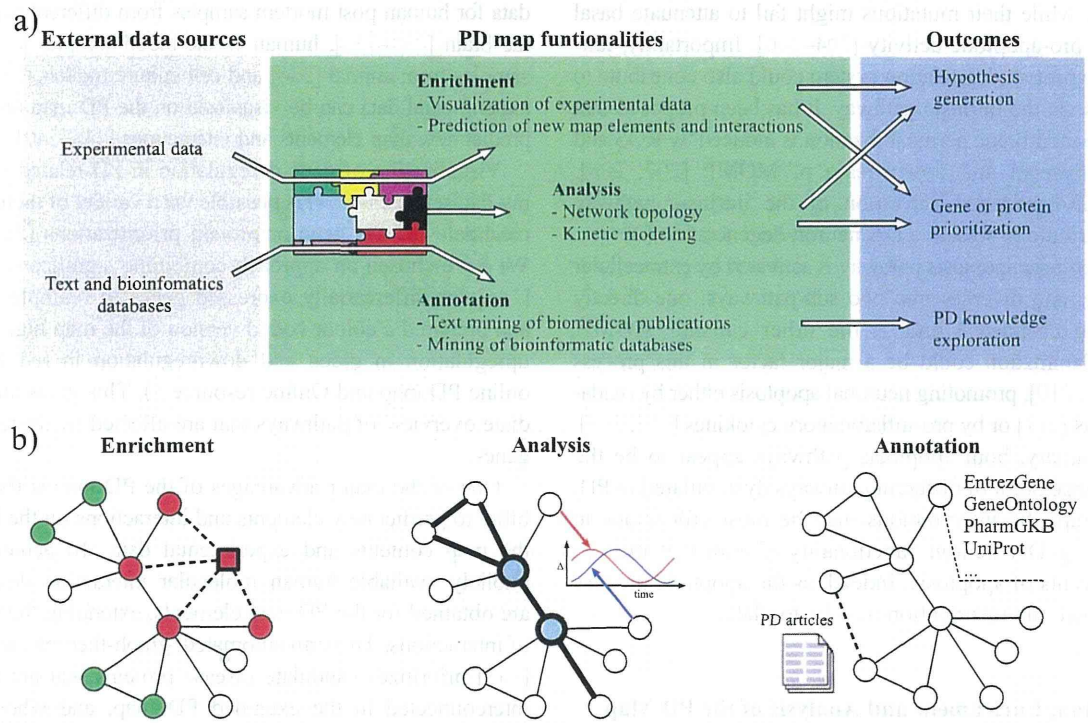

Fig. 3 The workflow and an illustration of PD map functionalities. **a** The PD map can be automatically enriched with experimental data and annotated with information from text and bioinformatics databases. The analysis requires no external data sources. **b** A simplified representation of the PD map is given, with *circles* (nodes) as map elements and *lines* (edges) as interactions (uni- or bi-directional). Enrichment: *green* and *red nodes* represent up- and downregulated genes, respectively, derived from experimental data; a predicted new map component (*square*) shares interaction with existing map components (*dashed lines*) and matches their expression profile. Analysis: nodes with high centrality (*blue*) play a key role in the network topology and indicate molecules regulating many processes; detection of paths (*thick lines*) highlights non-trivial relations between elements of a biological process; kinetic modelling reveals temporal dependencies between behaviour of different molecules. Annotation: text mining of PD-related articles suggests new interactions in the map (*thick dashed line*) and facilitates handling of a huge number of publications; each map element is annotated with information from various bioinformatics databases giving easy access to information about interesting elements

the network indicates a how given molecule, complex or interaction can affect communication between modules [248, 249]. More advanced, functional dependencies between elements in the network can be revealed by methods exploring the relationships of all possible paths between network elements and selected molecular dysfunctions [250] (see Fig. 3b for illustration). Examples of network analysis applied to the PD map can be found in Online resource 1.

Most of the connections on the PD map depict real physical interactions between biomolecules. Currently, the PD map contains no information on kinetics of these interactions; however, they can be easily assigned and analysed mathematically [251]. The PD map is compliant with the Systems Biology Markup Language (SBML) standard [252], used by commonly available software to build kinetic models and run simulations [253]. Although assigning kinetic parameters to all interactions in the PD map is a truly challenging task, describing kinetics of a certain process representing a module within the PD map is feasible. In-depth analysis of the dynamics of a process can provide insight as to how elements of the process change quantitatively and over time (see Fig. 3b for illustration) and assess their influence on the related components in the map. This can lead to new hypotheses that are impossible to discover by visual examination or analysis of static network topology [254]. There are many successful examples, where similar bottom–up modelling has been applied to neurobiology related systems [255–258].

In summary, structural network analysis allows for detection of elements key to PD pathogenesis represented in the map. This can serve as a basis for new hypotheses and prioritization of targets for further investigation.

Conclusions and Perspectives

PD is a neurodegenerative disease involving a complex interplay of environmental and genetic factors. It becomes increasingly important to develop new approaches to organize and explore the exploding knowledge of this field. The PD map is a computer-based knowledge repository, representing diagrammatically

molecular mechanisms of PD in a structured and standardized way. It can be linked to bioinformatics tools facilitating exploration and updating the contents of the map using bioinformatic annotations.

The main insights into molecular pathology of PD come from studies on familial PD and GWAS. In the future, massive use of next-generation sequencing will provide even more data that might contribute to PD. The PD map facilitates integration and visualization of large experimental datasets, allowing analyzing them in the context of disease mechanisms.

Discovering causal factors of PD pathogenesis is difficult because molecular pathways dysregulated in neurodegeneration are interconnected and influence each other. Analysis of the topology and dynamics of molecular interactions within and across different pathways represented in the PD map may help to uncover key factors in PD pathology. For instance, the role of neuroinflammation in the pathological cascade in PD remains unclear, while the apoptosis, clearly a downstream factor of PD, involves other mechanisms implicated in PD, like protein degradation or mitochondrial quality control. Consequential steps of PD pathology can be elucidated by the global, systems level analysis of all implicated factors.

The map has reached substantial size and complexity. Keeping it up-to-date and refining it with limited resources will be a challenge. We foresee the PD map as a crowdsourcing project, where an interested and knowledgeable research community is engaged in solving a problem [259–262], similar to WikiPathways or Payao [263, 264], but focused on disease-related mechanisms. Thus, the PD community will easily explore and curate the PD-related knowledge in an online manner, ensuring that individual contributions are recognized.

Acknowledgments We are grateful to Angela Hogan for language correction assistance.

Conflict of interest The authors declare that they have no conflict of interest.

References

1. Obeso JA, Rodriguez-Oroz MC, Goetz CG et al (2010) Missing pieces in the Parkinson's disease puzzle. Nat Med 16:653–661. doi:10.1038/nm.2165
2. Caron E, Ghosh S, Matsuoka Y et al (2010) A comprehensive map of the mTOR signaling network. Mol Syst Biol 6:453. doi:10.1038/msb.2010.108
3. Mizuno S, Iijima R, Ogishima S et al (2012) AlzPathway: a comprehensive map of signaling pathways of Alzheimer's disease. BMC Syst Biol 6:52. doi:10.1186/1752-0509-6-52
4. Ghosh S, Matsuoka Y, Asai Y et al (2011) Software for systems biology: from tools to integrated platforms. Nat Rev Genet 12:821–832
5. Kitano H, Ghosh S, Matsuoka Y (2011) Social engineering for virtual "big science" in systems biology. Nat Chem Biol 7:323–326
6. Lees AJ, Hardy J, Revesz T (2009) Parkinson's disease. Lancet 373:2055–2066. doi:10.1016/S0140-6736(09)60492-X
7. Jankovic J (2008) Parkinson's disease: clinical features and diagnosis. J Neurol Neurosurg Psychiatry 79:368–376. doi:10.1136/jnnp.2007.131045
8. Meissner WG, Frasier M, Gasser T et al (2011) Priorities in Parkinson's disease research. Nat Rev Drug Disc 10:377–393. doi:10.1038/nrd3430
9. Dick FD, De Palma G, Ahmadi A et al (2007) Environmental risk factors for Parkinson's disease and parkinsonism: the Geoparkinson study. Occup Environ Med 64:666–672. doi:10.1136/oem.2006.027003
10. Goldman SM, Tanner CM, Oakes D et al (2006) Head injury and Parkinson's disease risk in twins. Ann Neurol 60:65–72. doi:10.1002/ana.20882
11. Ritz B, Ascherio A, Checkoway H et al (2007) Pooled analysis of tobacco use and risk of Parkinson disease. Arch Neurol 64:990–997. doi:10.1001/archneur.64.7.990
12. Hu G, Bidel S, Jousilahti P et al (2007) Coffee and tea consumption and the risk of Parkinson's disease. Mov Disord 22:2242–2248. doi:10.1002/mds.21706
13. Saunders-Pullman R (2003) Estrogens and Parkinson disease: neuroprotective, symptomatic, neither, or both? Endocrine 21:81–87. doi:10.1385/ENDO:21:1:81
14. Klein C, Westenberger A (2012) Genetics of Parkinson's disease. Cold Spring Harb Perspect Med 2:a008888. doi:10.1101/cshperspect.a008888
15. Marques SCF, Oliveira CR, Pereira CMF, Outeiro TF (2011) Epigenetics in neurodegeneration: a new layer of complexity. Prog Neuropsychopharmacol Biol Psychiatry 35:348–355. doi:10.1016/j.pnpbp.2010.08.008
16. Migliore L, Coppedè F (2009) Genetics, environmental factors and the emerging role of epigenetics in neurodegenerative diseases. Mutat Res 667:82–97. doi:10.1016/j.mrfmmm.2008.10.011
17. Schapira AHV (2011) Aetiopathogenesis of Parkinson's disease. J Neurol 258:S307–S310. doi:10.1007/s00415-011-6016-y
18. Priyadarshi A, Khuder SA, Schaub EA, Priyadarshi SS (2001) Environmental risk factors and Parkinson's disease: a metaanalysis. Environ Res 86:122–127. doi:10.1006/enrs.2001.4264
19. Dick FD (2006) Parkinson's disease and pesticide exposures. Br Med Bull 79–80:219–231. doi:10.1093/bmb/ldl018
20. Davis GC, Williams AC, Markey SP et al (1979) Chronic Parkinsonism secondary to intravenous injection of meperidine analogues. Psychiatry Res 1:249–254
21. Langston JW, Ballard P, Tetrud JW, Irwin I (1983) Chronic Parkinsonism in humans due to a product of meperidine-analog synthesis. Science 219:979–980
22. Betarbet R, Sherer TB, MacKenzie G et al (2000) Chronic systemic pesticide exposure reproduces features of Parkinson's disease. Nat Neurosci 3:1301–1306. doi:10.1038/81834
23. Thiruchelvam M, Richfield EK, Baggs RB et al (2000) The nigrostriatal dopaminergic system as a preferential target of repeated exposures to combined paraquat and maneb: implications for Parkinson's disease. J Neurosci 20:9207–9214
24. Gash DM, Rutland K, Hudson NL et al (2008) Trichloroethylene: Parkinsonism and complex 1 mitochondrial neurotoxicity. Ann Neurol 63:184–192. doi:10.1002/ana.21288
25. Goldman SM (2010) Trichloroethylene and Parkinson's disease: dissolving the puzzle. Expert Rev Neurother 10:835–837. doi:10.1586/ern.10.61

26. Braak H, Del Tredici K, Rüb U et al (2003) Staging of brain pathology related to sporadic Parkinson's disease. Neurobiol Aging 24:197–211
27. Poulopoulos M, Levy OA, Alcalay RN (2012) The neuropathology of genetic Parkinson's disease. Mov Disord 000:1–12. doi:10.1002/mds.24962
28. Wolters EC (2009) Non-motor extranigral signs and symptoms in Parkinson's disease. Parkinsonism & Relat Disord 15(Suppl 3): S6–S12. doi:10.1016/S1353-8020(09)70770-9
29. Ferrer I, López-Gonzalez I, Carmona M et al (2012) Neurochemistry and the non-motor aspects of PD. Neurobiol Dis 46:508–526. doi:10.1016/j.nbd.2011.10.019
30. Sulzer D (2007) Multiple hit hypotheses for dopamine neuron loss in Parkinson's disease. Trends Neurosci 30:244–250. doi:10.1016/j.tins.2007.03.009
31. Matsuda W, Furuta T, Nakamura KC et al (2009) Single nigrostriatal dopaminergic neurons form widely spread and highly dense axonal arborizations in the neostriatum. J Neurosci 29:444–453
32. Matsuda W (2012) Imaging of dopaminergic neurons and the implications for Parkinson's disease. Syst Biol Parkinson's Dis. doi:10.1007/978-1-4614-3411-5
33. Parent M, Parent A (2006) Relationship between axonal collateralization and neuronal degeneration in basal ganglia. J Neural Transm Suppl 85–8
34. Schmitz Y, Luccarelli J, Kim M et al (2009) Glutamate controls growth rate and branching of dopaminergic axons. J Neurosci 29:11973–11981. doi:10.1523/JNEUROSCI.2927-09.2009
35. Braak H, Bohl JR, Müller CM et al (2006) Stanley Fahn Lecture 2005: the staging procedure for the inclusion body pathology associated with sporadic Parkinson's disease reconsidered. Mov Disord 21:2042–2051. doi:10.1002/mds.21065
36. Kim-Han JS, Antenor-Dorsey JA, O'Malley KL (2011) The Parkinsonian mimetic, MPP+, specifically impairs mitochondrial transport in dopamine axons. J Neurosci 31:7212–7221. doi:10.1523/JNEUROSCI.0711-11.2011
37. Dauer W, Przedborski S (2003) Parkinson's disease: mechanisms and models. Neuron 39:889–909
38. Chan CS, Guzman JN, Ilijic E et al (2007) "Rejuvenation" protects neurons in mouse models of Parkinson's disease. Nature 447:1081–1086. doi:10.1038/nature05865
39. Surmeier DJ, Guzman JN, Sanchez-Padilla J, Schumacker PT (2011) The role of calcium and mitochondrial oxidant stress in the loss of substantia nigra pars compacta dopaminergic neurons in Parkinson's disease. Neuroscience 198:221–231
40. Asanuma M, Miyazaki I, Ogawa N (2003) Dopamine- or L-DOPA-induced neurotoxicity: the role of dopamine quinone formation and tyrosinase in a model of Parkinson's disease. Neurotox Res 5:165–176
41. Cantuti-Castelvetri I, Shukitt-Hale B, Joseph JA (2003) Dopamine neurotoxicity: age-dependent behavioral and histological effects. Neurobiol aging 24:697–706
42. Collier TJ, Kanaan NM, Kordower JH (2011) Ageing as a primary risk factor for Parkinson's disease: evidence from studies of non-human primates. Nat Rev Neurosci 12:359–366. doi:10.1038/nrn3039
43. Mosharov EV, Larsen KE, Kanter E et al (2009) Interplay between cytosolic dopamine, calcium, and alpha-synuclein causes selective death of substantia nigra neurons. Neuron 62:218–229. doi:10.1016/j.neuron.2009.01.033
44. Rubinsztein DC, Mariño G, Kroemer G (2011) Autophagy and aging. Cell 146:682–695. doi:10.1016/j.cell.2011.07.030
45. Mammucari C, Rizzuto R (2010) Signaling pathways in mitochondrial dysfunction and aging. Mech Ageing Dev 131:536–543. doi:10.1016/j.mad.2010.07.003
46. Green DR, Galluzzi L, Kroemer G (2011) Mitochondria and the autophagy–inflammation–cell death axis in organismal aging. Science 333:1109–1112. doi:10.1126/science.1201940
47. Venkateshappa C, Harish G, Mythri RB et al (2012) Increased oxidative damage and decreased antioxidant function in aging human substantia nigra compared to striatum: implications for Parkinson's disease. Neurochem Res 37:358–369. doi:10.1007/s11064-011-0619-7
48. Mallucci GR (2009) Prion neurodegeneration: starts and stops at the synapse. Prion 3:195–201
49. Sisková Z, Sanyal NK, Orban A et al (2010) Reactive hypertrophy of synaptic varicosities within the hippocampus of prion-infected mice. Biochem Soc Trans 38:471–475
50. Masliah E (1998) Mechanisms of synaptic pathology in Alzheimer's disease. J Neural Transm Suppl 53:147–158
51. Palop JJ, Mucke L (2010) Amyloid-beta-induced neuronal dysfunction in Alzheimer's disease: from synapses toward neural networks. Nat Neurosci 13:812–818
52. Polymeropoulos MH, Lavedan C, Leroy E et al (1997) Mutation in the alpha-synuclein gene identified in families with Parkinson's disease. Science 276:2045–2047
53. Singleton AB, Farrer MJ, Johnson J et al (2003) alpha-Synuclein locus triplication causes Parkinson's disease. Science 302:841. doi:10.1126/science.1090278
54. Simón-Sánchez J, Schulte C, Bras JM et al (2009) Genome-wide association study reveals genetic risk underlying Parkinson's disease. Nat Genet 41:1308–1312
55. Fortin DL, Nemani VM, Voglmaier SM et al (2005) Neural activity controls the synaptic accumulation of alpha-synuclein. J Neurosci 25:10913–10921. doi:10.1523/JNEUROSCI.2922-05.2005
56. Burré J, Sharma M, Tsetsenis T et al (2010) Alpha-synuclein promotes SNARE-complex assembly in vivo and in vitro. Science 329:1663–1667
57. Chandra S, Gallardo G, Fernández-Chacón R et al (2005) Alpha-synuclein cooperates with CSPalpha in preventing neurodegeneration. Cell 123:383–396
58. Quilty MC, King AE, Gai W-P et al (2006) Alpha-synuclein is upregulated in neurones in response to chronic oxidative stress and is associated with neuroprotection. Exp Neurol 199:249–256
59. Nemani VM, Lu W, Berge V et al (2010) Increased expression of alpha-synuclein reduces neurotransmitter release by inhibiting synaptic vesicle reclustering after endocytosis. Neuron 65:66–79
60. Schulz-Schaeffer WJ (2010) The synaptic pathology of α-synuclein aggregation in dementia with Lewy bodies, Parkinson's disease and Parkinson's disease dementia. Acta Neuropathologica 120:131–143
61. Piccoli G, Condliffe SB, Bauer M et al (2011) LRRK2 controls synaptic vesicle storage and mobilization within the recycling pool. J Neurosci 31:2225–2237
62. Shin N, Jeong H, Kwon J et al (2008) LRRK2 regulates synaptic vesicle endocytosis. Exp Cell Res 314:2055–2065
63. Conway KA, Rochet JC, Bieganski RM, Lansbury PT (2001) Kinetic stabilization of the alpha-synuclein protofibril by a dopamine-alpha-synuclein adduct. Science 294:1346–1349. doi:10.1126/science.1063522
64. Leong SL, Cappai R, Barnham KJ, Pham CLL (2009) Modulation of alpha-synuclein aggregation by dopamine: a review. Neurochem Res 34:1838–1846
65. Perier C, Vila M (2012) Mitochondrial biology and Parkinson's disease. Cold Spring Harb Perspect Med 2:a009332. doi:10.1101/cshperspect.a009332
66. Tai H-C, Schuman EM (2008) Ubiquitin, the proteasome and protein degradation in neuronal function and dysfunction. Nat Rev Neurosci 9:826–838
67. Youle RJ, Van der Bliek AM (2012) Mitochondrial fission, fusion, and stress. Science 337:1062–1065. doi:10.1126/science.1219855
68. Schapira AHV, Cooper JM, Dexter D et al (1990) Mitochondrial complex I deficiency in Parkinson's disease. J Neurochem 54: 823–827

69. Parker WD, Boyson SJ, Parks JK (1989) Abnormalities of the electron transport chain in idiopathic Parkinson's disease. Ann Neurol 26:719–723. doi:10.1002/ana.410260606
70. Koopman W, Willems P (2012) Monogenic mitochondrial disorders. New Engl J Med
71. Matsuda N, Sato S, Shiba K et al (2010) PINK1 stabilized by mitochondrial depolarization recruits Parkin to damaged mitochondria and activates latent Parkin for mitophagy. J Cell Biol 189:211–221. doi:10.1083/jcb.200910140
72. Plun-Favreau H, Klupsch K, Moisoi N et al (2007) The mitochondrial protease HtrA2 is regulated by Parkinson's disease-associated kinase PINK1. Nature Cell Biol 9:1243–1252. doi:10.1038/ncb1644
73. Pridgeon JW, Olzmann J a, Chin L-S, Li L (2007) PINK1 protects against oxidative stress by phosphorylating mitochondrial chaperone TRAP1. PLoS Biol 5:e172. doi:10.1371/journal.pbio.0050172
74. Chan NC, Salazar AM, Pham AH et al (2011) Broad activation of the ubiquitin–proteasome system by Parkin is critical for mitophagy. Hum Mol Genet 20:1726–1737. doi:10.1093/hmg/ddr048
75. Gegg ME, Cooper JM, Chau K-Y et al (2010) Mitofusin 1 and mitofusin 2 are ubiquitinated in a PINK1/parkin-dependent manner upon induction of mitophagy. Hum Mol Genet 19:4861–4870. doi:10.1093/hmg/ddq419
76. Geisler S, Holmström KM, Skujat D et al (2010) PINK1/Parkin-mediated mitophagy is dependent on VDAC1 and p62/SQSTM1. Nature Cell Biol 12:119–131. doi:10.1038/ncb2012
77. Shin J-H, Ko HS, Kang H et al (2011) PARIS (ZNF746) Repression of PGC-1α contributes to neurodegeneration in Parkinson's disease. Cell 144:689–702. doi:10.1016/j.cell.2011.02.010
78. Scarpulla RC (2008) Transcriptional paradigms in mammalian mitochondrial biogenesis and function. Physiol Rev 88:611–638. doi:10.1152/physrev.00025.2007
79. Ryan MT, Hoogenraad NJ (2007) Mitochondrial-nuclear communications. Annu Rev Biochem 76:701–722. doi:10.1146/annurev.biochem.76.052305.091720
80. Gandhi S, Wood-Kaczmar A, Yao Z et al (2009) PINK1-associated Parkinson's disease is caused by neuronal vulnerability to calcium-induced cell death. Molecular Cell 33:627–638. doi:10.1016/j.molcel.2009.02.013
81. Yao Z, Gandhi S, Burchell VS et al (2011) Cell metabolism affects selective vulnerability in PINK1-associated Parkinson's disease. J Cell Sci 124:4194–4202. doi:10.1242/jcs.088260
82. Tschopp J (2011) Mitochondria: Sovereign of inflammation? Eur J Immunol 41:1196–1202
83. Thomas KJ, McCoy MK, Blackinton J et al (2011) DJ-1 acts in parallel to the PINK1/parkin pathway to control mitochondrial function and autophagy. Hum Mol Genet 20:40–50. doi:10.1093/hmg/ddq430
84. Burbulla LF, Schelling C, Kato H et al (2010) Dissecting the role of the mitochondrial chaperone mortalin in Parkinson's disease: functional impact of disease-related variants on mitochondrial homeostasis. Hum Mol Genet 19:4437–4452. doi:10.1093/hmg/ddq370
85. Yang H, Zhou X, Liu X et al (2011) Mitochondrial dysfunction induced by knockdown of mortalin is rescued by Parkin. Biochem Biophys Res Commun 410:114–120. doi:10.1016/j.bbrc.2011.05.116
86. Weihofen A, Thomas KJ, Ostaszewski BL et al (2009) Pink1 forms a multiprotein complex with Miro and Milton, linking Pink1 function to mitochondrial trafficking. Biochemistry 48:2045–2052. doi:10.1021/bi8019178
87. Wang X, Winter D, Ashrafi G et al (2011) PINK1 and Parkin target Miro for phosphorylation and degradation to arrest mitochondrial motility. Cell 147:893–906. doi:10.1016/j.cell.2011.10.018
88. Pilsl A, Winklhofer KF (2012) Parkin, PINK1 and mitochondrial integrity: emerging concepts of mitochondrial dysfunction in Parkinson's disease. Acta Neuropathol 123:173–188. doi:10.1007/s00401-011-0902-3
89. Sheng Z-H, Cai Q (2012) Mitochondrial transport in neurons: impact on synaptic homeostasis and neurodegeneration. Nat Rev Neurosci 13:77–93. doi:10.1038/nrn3156
90. Lee H-J, Khoshaghideh F, Lee S, Lee S-J (2006) Impairment of microtubule-dependent trafficking by overexpression of alpha-synuclein. Eur J Neurosci 24:3153–3162. doi:10.1111/j.1460-9568.2006.05210.x
91. Yang F, Jiang Q, Zhao J et al (2005) Parkin stabilizes microtubules through strong binding mediated by three independent domains. J Biol Chem 280:17154–17162. doi:10.1074/jbc.M500843200
92. Gillardon F (2009) Leucine-rich repeat kinase 2 phosphorylates brain tubulin-beta isoforms and modulates microtubule stability—a point of convergence in parkinsonian neurodegeneration? J Neurochem 110:1514–1522. doi:10.1111/j.1471-4159.2009.06235.x
93. Borland MK, Trimmer PA, Rubinstein JD et al (2008) Chronic, low-dose rotenone reproduces Lewy neurites found in early stages of Parkinson's disease, reduces mitochondrial movement and slowly kills differentiated SH-SY5Y neural cells. Mol Neurodegener 3:21. doi:10.1186/1750-1326-3-21
94. Park D-W, Nam M-K, Rhim H (2011) The serine protease HtrA2 cleaves UCH-L1 and inhibits its hydrolase activity: implication in the UCH-L1-mediated cell death. Biochem Biophys Res Commun 415:24–29. doi:10.1016/j.bbrc.2011.09.148
95. Gusdon AM, Zhu J, Van Houten B, Chu CT (2012) ATP13A2 regulates mitochondrial bioenergetics through macroautophagy. Neurobiol Dis 45:962–972. doi:10.1016/j.nbd.2011.12.015
96. Braschi E, Goyon V, Zunino R et al (2010) Vps35 mediates vesicle transport between the mitochondria and peroxisomes. Curr Biol 20:1310–1315. doi:10.1016/j.cub.2010.05.066
97. Chartier-Harlin M-C, Dachsel JC, Vilariño-Güell C et al (2011) Translation initiator EIF4G1 mutations in familial Parkinson disease. Am J Hum Genet 89:398–406. doi:10.1016/j.ajhg.2011.08.009
98. Lee J, Giordano S, Zhang J (2012) Autophagy, mitochondria and oxidative stress: cross-talk and redox signalling. Biochem J 441:523–540. doi:10.1042/BJ20111451
99. Korolchuk VI, Menzies FM, Rubinsztein DC (2010) Mechanisms of cross-talk between the ubiquitin–proteasome and autophagy–lysosome systems. FEBS Lett 584:1393–1398
100. Kroemer G, Mariño G, Levine B (2010) Autophagy and the integrated stress response. Molecular cell 40:280–293. doi:10.1016/j.molcel.2010.09.023
101. Ravikumar B, Sarkar S, Davies JE et al (2010) Regulation of mammalian autophagy in physiology and pathophysiology. Physiol Rev 90:1383–1435. doi:10.1152/physrev.00030.2009
102. Harris H, Rubinsztein DC (2011) Control of autophagy as a therapy for neurodegenerative disease. Nat Rev Neurol 8:108–117. doi:10.1038/nrneurol.2011.200
103. Martinez-Vicente M, Talloczy Z, Kaushik S et al (2008) Dopamine-modified alpha-synuclein blocks chaperone-mediated autophagy. J Clin Investig 118:777–788. doi:10.1172/JCI32806DS1
104. Nalls MA, Plagnol V, Hernandez DG et al (2011) Imputation of sequence variants for identification of genetic risks for Parkinson's disease: a meta-analysis of genome-wide association studies. Lancet 377:641–649
105. Grabowski GA (2008) Phenotype, diagnosis, and treatment of Gaucher's disease. Lancet 372:1263–1271
106. Yap TL, Gruschus JM, Velayati A et al (2011) {alpha}-Synuclein interacts with glucocerebrosidase providing a molecular link between Parkinson and Gaucher diseases. J Biol Chem 286:28080–28088. doi:10.1074/jbc.M111.237859
107. Westbroek W, Gustafson AM, Sidransky E (2011) Exploring the link between glucocerebrosidase mutations and parkinsonism. Trends Mol Med 17:485–493

108. Alvarez-Erviti L, Rodriguez-Oroz MC, Cooper JM et al (2010) Chaperone-mediated autophagy markers in Parkinson disease brains. Arch Neurol 67:1464–1472
109. Crews L, Spencer B, Desplats P et al (2010) Selective molecular alterations in the autophagy pathway in patients with Lewy body disease and in models of alpha-synucleinopathy. PLoS One 5:e9313
110. Chu Y, Dodiya H, Aebischer P et al (2009) Alterations in lysosomal and proteasomal markers in Parkinson's disease: relationship to alpha-synuclein inclusions. Neurobiol Dis 35:385–398. doi:10.1016/j.nbd.2009.05.023
111. Xu M, Zhang H (2011) Death and survival of neuronal and astrocytic cells in ischemic brain injury: a role of autophagy. Acta Pharmacol Sin 32:1089–1099
112. Chu CT (2006) Autophagic stress in neuronal injury and disease. J Neuropathol Exp Neurol 65:423–432
113. Schapira AHV (2012) Targeting mitochondria for neuroprotection in Parkinson's disease. Antioxid Redox Signal 16:965–973. doi:10.1089/ars.2011.4419
114. Nixon RA, Yang D-S (2011) Autophagy failure in Alzheimer's disease—locating the primary defect. Neurobiol Dis 43:38–45. doi:10.1016/j.nbd.2011.01.021
115. Pickford F, Masliah E, Britschgi M et al (2008) The autophagy-related protein beclin 1 shows reduced expression in early Alzheimer disease and regulates amyloid beta accumulation in mice. J Clin Investig 118:2190–2199
116. Yang D-S, Stavrides P, Mohan PS et al (2011) Therapeutic effects of remediating autophagy failure in a mouse model of Alzheimer disease by enhancing lysosomal proteolysis. Autophagy 7:788–789
117. Komatsu M, Waguri S, Chiba T et al (2006) Loss of autophagy in the central nervous system causes neurodegeneration in mice. Nature 441:880–884. doi:10.1038/nature04723
118. Hara T, Nakamura K, Matsui M et al (2006) Suppression of basal autophagy in neural cells causes neurodegenerative disease in mice. Nature 441:885–889. doi:10.1038/nature04724
119. Breydo L, Wu JW, Uversky VN (2012) α-Synuclein misfolding and Parkinson's disease. Biochim Biophys Acta 1822:261–285. doi:10.1016/j.bbadis.2011.10.002
120. Ullman O, Fisher CK, Stultz CM (2011) Explaining the structural plasticity of α-synuclein. J Am Chem Soc 133:19536–19546
121. Wang W, Perovic I, Chittuluru J et al (2011) A soluble α-synuclein construct forms a dynamic tetramer. PNAS 108:17797–17802
122. Bartels T, Choi JG, Selkoe DJ (2011) α-Synuclein occurs physiologically as a helically folded tetramer that resists aggregation. Nature 3–7. doi: 10.1038/nature10324
123. Lee S-J, Lim H-S, Masliah E, Lee H-J (2011) Protein aggregate spreading in neurodegenerative diseases: Problems and perspectives. Neurosci Res 70:339–348
124. Yonetani M, Nonaka T, Masuda M et al (2009) Conversion of wild-type alpha-synuclein into mutant-type fibrils and its propagation in the presence of A30P mutant. J Biol Chem 284:7940–7950
125. Colla E, Jensen PH, Pletnikova O et al (2012) Accumulation of toxic α-synuclein oligomer within endoplasmic reticulum occurs in α-synucleinopathy in vivo. J Neurosci 32:3301–3305. doi:10.1523/JNEUROSCI.5368-11.2012
126. Chung CY, Koprich JB, Siddiqi H, Isacson O (2009) Dynamic changes in presynaptic and axonal transport proteins combined with striatal neuroinflammation precede dopaminergic neuronal loss in a rat model of AAV alpha-synucleinopathy. J Neurosci 29:3365–3373. doi:10.1523/JNEUROSCI.5427-08.2009
127. Ihara M, Yamasaki N, Hagiwara A et al (2007) Sept4, a component of presynaptic scaffold and Lewy bodies, is required for the suppression of alpha-synuclein neurotoxicity. Neuron 53:519–533. doi:10.1016/j.neuron.2007.01.019
128. Kahle PJ, Neumann M, Ozmen L et al (2000) Subcellular localization of wild-type and Parkinson's disease-associated mutant alpha-synuclein in human and transgenic mouse brain. J Neurosci 20:6365–6373
129. Yavich L, Jäkälä P, Tanila H (2006) Abnormal compartmentalization of norepinephrine in mouse dentate gyrus in alpha-synuclein knockout and A30P transgenic mice. J Neurochem 99:724–732. doi:10.1111/j.1471-4159.2006.04098.x
130. Martin LJ, Pan Y, Price AC et al (2006) Parkinson's disease alpha-synuclein transgenic mice develop neuronal mitochondrial degeneration and cell death. J Neurosci 26:41–50. doi:10.1523/JNEUROSCI.4308-05.2006
131. Devi L, Raghavendran V, Prabhu BM et al (2008) Mitochondrial import and accumulation of alpha-synuclein impair complex I in human dopaminergic neuronal cultures and Parkinson disease brain. J Biol Chem 283:9089–9100. doi:10.1074/jbc.M710012200
132. Loeb V, Yakunin E, Saada A, Sharon R (2010) The transgenic overexpression of alpha-synuclein and not its related pathology associates with complex I inhibition. J Biol Chem 285:7334–7343. doi:10.1074/jbc.M109.061051
133. Chinta SJ, Mallajosyula JK, Rane A, Andersen JK (2010) Mitochondrial alpha-synuclein accumulation impairs complex I function in dopaminergic neurons and results in increased mitophagy in vivo. Neurosci Lett 486:235–239. doi:10.1016/j.neulet.2010.09.061
134. Choubey V, Safiulina D, Vaarmann A et al (2011) Mutant A53T alpha-synuclein induces neuronal death by increasing mitochondrial autophagy. J Biol Chem 286:10814–10824. doi:10.1074/jbc.M110.132514
135. Esposito A, Dohm CP, Kermer P et al (2007) alpha-Synuclein and its disease-related mutants interact differentially with the microtubule protein tau and associate with the actin cytoskeleton. Neurobiol Dis 26:521–531. doi:10.1016/j.nbd.2007.01.014
136. Lee H-J, Shin SY, Choi C et al (2002) Formation and removal of alpha-synuclein aggregates in cells exposed to mitochondrial inhibitors. J Biol Chem 277:5411–5417. doi:10.1074/jbc.M105326200
137. Chen L, Jin J, Davis J et al (2007) Oligomeric α-synuclein inhibits tubulin polymerization. Biochem Biophys Res Commun 356:548–553. doi:10.1016/j.bbrc.2007.02.163
138. Jensen PH (1999) alpha -Synuclein binds to tau and stimulates the protein kinase A-catalyzed tau phosphorylation of serine residues 262 and 356. J Biol Chem 274:25481–25489. doi:10.1074/jbc.274.36.25481
139. Frasier M, Walzer M, McCarthy L et al (2005) Tau phosphorylation increases in symptomatic mice overexpressing A30P alpha-synuclein. Exp Neurol 192:274–287. doi:10.1016/j.expneurol.2004.07.016
140. Haggerty T, Credle J, Rodriguez O et al (2011) Hyperphosphorylated Tau in an α-synuclein-overexpressing transgenic model of Parkinson's disease. Eur J Neurosci 33:1598–1610. doi:10.1111/j.1460-9568.2011.07660.x
141. Qureshi HY, Paudel HK (2011) Parkinsonian neurotoxin 1-methyl-4-phenyl-1,2,3,6-tetrahydropyridine (MPTP) and alpha-synuclein mutations promote Tau protein phosphorylation at Ser262 and destabilize microtubule cytoskeleton in vitro. J Biol Chem 286:5055–5068. doi:10.1074/jbc.M110.178905
142. Clinton LK, Blurton-Jones M, Myczek K et al (2010) Synergistic interactions between Abeta, tau, and alpha-synuclein: acceleration of neuropathology and cognitive decline. J Neurosci 30:7281–7289
143. Giasson BI, Forman MS, Higuchi M et al (2003) Initiation and synergistic fibrillization of tau and alpha-synuclein. Science 300:636–640. doi:10.1126/science.1082324
144. Smith WW, Jiang H, Pei Z et al (2005) Endoplasmic reticulum stress and mitochondrial cell death pathways mediate A53T mutant alpha-synuclein-induced toxicity. Hum Mol Genet 14:3801–3811. doi:10.1093/hmg/ddi396
145. Colla E, Coune P, Liu Y et al (2012) Endoplasmic reticulum stress is important for the manifestations of α-synucleinopathy in vivo. J Neurosci 32:3306–3320

146. Cuervo AM, Stefanis L, Fredenburg R et al (2004) Impaired degradation of mutant alpha-synuclein by chaperone-mediated autophagy. Science 305:1292–1295. doi:10.1126/science.1101738
147. Xilouri M, Vogiatzi T, Vekrellis K et al (2009) Abberant alpha-synuclein confers toxicity to neurons in part through inhibition of chaperone-mediated autophagy. PLoS One 4:e5515. doi:10.1371/journal.pone.0005515
148. Mazzulli JR, Xu Y-H, Sun Y et al (2011) Gaucher disease glucocerebrosidase and α-synuclein form a bidirectional pathogenic loop in synucleinopathies. Cell 146:37–52. doi:10.1016/j.cell.2011.06.001
149. Tanaka Y, Engelender S, Igarashi S et al (2001) Inducible expression of mutant alpha-synuclein decreases proteasome activity and increases sensitivity to mitochondria-dependent apoptosis. Hum Mol Genet 10:919–926. doi:10.1093/hmg/10.9.919
150. Stefanis L, Larsen KE, Rideout HJ et al (2001) Expression of A53T mutant but not wild-type alpha-synuclein in PC12 cells induces alterations of the ubiquitin-dependent degradation system, loss of dopamine release, and autophagic cell death. J Neurosci 21:9549–9560
151. Petrucelli L, O'Farrell C, Lockhart PJ et al (2002) Parkin protects against the toxicity associated with mutant α-synuclein proteasome dysfunction selectively affects catecholaminergic neurons. Neuron 36:1007–1019. doi:10.1016/S0896-6273(02)01125-X
152. Lindersson E, Beedholm R, Højrup P et al (2004) Proteasomal inhibition by alpha-synuclein filaments and oligomers. J Biol Chem 279:12924–12934. doi:10.1074/jbc.M306390200
153. Goedert M, Clavaguera F, Tolnay M (2010) The propagation of prion-like protein inclusions in neurodegenerative diseases. Trends Neurosci 33:317–325
154. Kordower JH, Chu Y, Hauser RA et al (2008) Lewy body-like pathology in long-term embryonic nigral transplants in Parkinson's disease. Nature Medicine 14:504–506. doi:10.1038/nm1747
155. Kordower JH, Chu Y, Hauser RA et al (2008) Transplanted dopaminergic neurons develop PD pathologic changes: a second case report. Mov Disord 23:2303–2306
156. Li J-Y, Englund E, Holton JL et al (2008) Lewy bodies in grafted neurons in subjects with Parkinson's disease suggest host-to-graft disease propagation. Nature Medicine 14:501–503. doi:10.1038/nm1746
157. Desplats P, Lee H-J, Bae E-J et al (2009) Inclusion formation and neuronal cell death through neuron-to-neuron transmission of alpha-synuclein. PNAS 106:13010–13015. doi:10.1073/pnas.0903691106
158. Volpicelli-Daley LA, Luk KC, Patel TP et al (2011) Exogenous α-synuclein fibrils induce Lewy body pathology leading to synaptic dysfunction and neuron death. Neuron 72:57–71
159. Luk KC, Kehm V, Carroll J et al (2012) Pathological α-synuclein transmission initiates Parkinson-like neurodegeneration in nontransgenic mice. Science 338:949–953. doi:10.1126/science.1227157
160. Jang A, Lee H-J, Suk J-E et al (2010) Non-classical exocytosis of alpha-synuclein is sensitive to folding states and promoted under stress conditions. J Neurochem 113:1263–1274
161. Lee H-J, Patel S, Lee S-J (2005) Intravesicular localization and exocytosis of alpha-synuclein and its aggregates. J Neurosci 25:6016–6024
162. Luk KC, Song C, O'Brien P et al (2009) Exogenous alpha-synuclein fibrils seed the formation of Lewy body-like intracellular inclusions in cultured cells. PNAS 106:20051–20056
163. Mosley RL, Hutter-Saunders JA, Stone DK, Gendelman HE (2012) Inflammation and adaptive immunity in Parkinson's disease. Cold Spring Harbor perspectives in medicine 2:a009381.
164. McGeer PL, Itagaki S, Akiyama H, McGeer EG (1988) Rate of cell death in parkinsonism indicates active neuropathological process. Ann Neurol 24:574–576
165. Brochard V, Combadière B, Prigent A et al (2009) Infiltration of CD4+ lymphocytes into the brain contributes to neurodegeneration in a mouse model of Parkinson disease. J Clin Investig 119:182–192. doi:10.1172/JCI36470
166. Double KL, Rowe DB, Carew-Jones FM et al (2009) Anti-melanin antibodies are increased in sera in Parkinson's disease. Exp Neurol 217:297–301. doi:10.1016/j.expneurol.2009.03.002
167. Reynolds AD, Stone DK, Hutter J a L et al (2010) Regulatory T cells attenuate Th17 cell-mediated nigrostriatal dopaminergic neurodegeneration in a model of Parkinson's disease. J Immunol 184:2261–2271. doi:10.4049/jimmunol.0901852, Baltimore, Md: 1950
168. Lucin KM, Wyss-Coray T (2009) Immune activation in brain aging and neurodegeneration: too much or too little? Neuron 64:110–122
169. Glass CK, Saijo K, Winner B et al (2010) Mechanisms underlying inflammation in neurodegeneration. Cell 140:918–934. doi:10.1016/j.cell.2010.02.016
170. Rocha SM, Cristovão AC, Campos FL et al (2012) Astrocyte-derived GDNF is a potent inhibitor of microglial activation. Neurobiol Dis 47:407–415. doi:10.1016/j.nbd.2012.04.014
171. Nimmerjahn A, Kirchhoff F, Helmchen F (2005) Resting microglial cells are highly dynamic surveillants of brain parenchyma in vivo. Science 308:1314–1318
172. Davalos D, Grutzendler J, Yang G et al (2005) ATP mediates rapid microglial response to local brain injury in vivo. Nat Neurosci 8:752–758
173. Mott RT, Ait-Ghezala G, Town T et al (2004) Neuronal expression of CD22: novel mechanism for inhibiting microglial proinflammatory cytokine production. Glia 46:369–379
174. Majed HH, Chandran S, Niclou SP et al (2006) A novel role for Sema3A in neuroprotection from injury mediated by activated microglia. J Neurosci 26:1730–1738
175. Tian L, Rauvala H, Gahmberg CG (2009) Neuronal regulation of immune responses in the central nervous system. Trends Immunol 30:91–99
176. Koning N, Bö L, Hoek RM, Huitinga I (2007) Downregulation of macrophage inhibitory molecules in multiple sclerosis lesions. Ann Neurol 62:504–514
177. Cardona AE, Pioro EP, Sasse ME et al (2006) Control of microglial neurotoxicity by the fractalkine receptor. Nat Neurosci 9:917–924
178. Kim WG, Mohney RP, Wilson B et al (2000) Regional difference in susceptibility to lipopolysaccharide-induced neurotoxicity in the rat brain: role of microglia. J Neurosci: Off J Soc Neurosci 20:6309–6316
179. Mena M a, Yébenes G d J (2008) Immune activation in brain aging and neurodegeneration: too much or too little? Neuroscientist 14:544–560. doi:10.1177/1073858408322839
180. Zecca L, Wilms H, Geick S et al (2008) Human neuromelanin induces neuroinflammation and neurodegeneration in the rat substantia nigra: implications for Parkinson's disease. Acta Neuropathol 116:47–55. doi:10.1007/s00401-008-0361-7
181. McGeer PL, Itagaki S, Boyes BE, McGeer EG (1988) Reactive microglia are positive for HLA-DR in the substantia nigra of Parkinson's and Alzheimer's disease brains. Neurology 38:1285–1285
182. Langston JW, Forno LS, Tetrud J et al (1999) Evidence of active nerve cell degeneration in the substantia nigra of humans years after 1-methyl-4-phenyl-1,2,3,6-tetrahydropyridine exposure. Ann Neurol 46:598–605
183. McGeer PL, Schwab C, Parent A, Doudet D (2003) Presence of reactive microglia in monkey substantia nigra years after 1-methyl-4-phenyl-1,2,3,6-tetrahydropyridine administration. Ann Neurol 54:599–604. doi:10.1002/ana.10728
184. Czlonkowska A, Kohutnicka M, Kurkowska-Jastrzebska I, Czlonkowski A (1996) Microglial reaction in MPTP (1-methyl-4-phenyl-1,2,3,6-tetrahydropyridine) induced Parkinson's disease mice model. Neurodegeneration 5:137–143